

1 Manuscript type: Research article

2 **Assessing Landslide Damming susceptibility in Central Asia**

3 Carlo Tacconi Stefanelli^{a,b,*}, William Frodella^{a,b}, Francesco Caleca^{a,b}, Zhanar Raimbekova^{c,d},
4 Ruslan Umuraliev^{d,e}, Veronica Tofani^{a,b}

5 ^a University of Florence, Department of Earth Sciences, via G. la Pira 4, 50121 Florence, Italy

6 ^b UNESCO Chair on the Prevention and Sustainable Management of Geo-Hydrological Hazards, University of
7 Florence, Largo Fermi 2, 50125 Florence, Italy

8 ^c Institute of Seismology of Republic of Kazakhstan (IS), Almaty, Kazakhstan

9 ^d [Al-Farabi Kazakh National University, Department of Geography and Environmental Sciences, Al-Farabi ave.](#)
10 [71, A15E3C7 Almaty, Kazakhstan](#)

11 ^{d,e} Institute of Seismology of the National Academy of Sciences of Kyrgyz Republic (ISNASKR), Bishkek, Kyrgyz
12 Republic

13 * Correspondence to: carlo.tacconistefanelli@unifi.it

14 **Abstract**

15 Central Asia regions are characterized by active tectonics, high mountain chains with extreme topography with
16 glaciers and strong seasonal rainfall events. These key predisposing factors make large landslides a serious natural
17 threat in the area, causing several casualties every year. The mountain crests are divided by wide lenticular or
18 narrow, linear intermountain tectonic depressions, which are incised by many of the most important Central Asia
19 rivers and are also subject to major seasonal river flood hazard. This multi-hazard combination is a source of
20 potential damming scenarios which can bring cascading effects with devastating consequences for the surrounding
21 settlements and population. Different hazards can only be managed with a multi-hazard approach coherent within
22 the different countries, as suggested by the requirements of the Sendai Framework for Disaster Risk Reduction.

23 This work was carried out within the framework of the SFRARR Project (“*Strengthening Financial Resilience*
24 *and Accelerating Risk Reduction in Central Asia*”) as a part of a multi-hazard approach with the aim of providing
25 a damming susceptibility analysis at a regional scale for Central Asia. To achieve this, a semi-automated GIS-
26 based mapping method, centred on a bivariate correlation of morphometric parameters defined by a morphological
27 index, originally designed to assess the damming susceptibility at basin/regional scale, was modified to be adopted
28 nationwide and applied to spatially assess the obstruction of the river network in Central Asia for mapped and
29 newly formed landslides. The proposed methodology represents an improvement of the previously designed,
30 requiring a smaller amount of data, bringing new [preliminary](#) information on the damming hazard management
31 and risk reduction [identifying the most critical area within](#) ~~for~~ the Central Asia regions.

32 1 Introduction

33 The mountainous areas of the Djungaria, Tien Shan, Pamir and Kopetdag in Central Asia territories are
34 characterized by complex and active tectonic and are the sources of most of Central Asia rivers. A rugged
35 topography along with complex geological structure and high seismicity are ideal setting for large slope failures.
36 In general, when landslides completely obstruct a river channel, they generate a landslide dam whose consequences
37 can be a serious hazard forming upstream backwater and causing catastrophic downstream flooding, changes in
38 the riverbed-course, embankments instability triggering other landslides with a cascading effect (Swanson et al.,
39 1986; Costa and Schuster, 1988; Casagli and Ermini, 1999). The effects of impounded water and anomalous flood
40 waves, resulting from a dam breach, have significant economic and social impacts in upstream and downstream
41 areas with economic and human losses (King et al., 1989; Dai et al., 2005; Chen and Chang, 2016). Rebuilding
42 costs can be extensive, as they are direct (e.g., infrastructure and buildings reconstruction, safety measures) and
43 indirect (e.g., loss in real estate value and damage caused to industrial and agricultural production), harder to
44 estimate.

45 Most of landslide dams have a short life as about 40% of them collapse within 24 hours after formation and about
46 80% within one year (Costa and Schuster, 1988; Tacconi Stefanelli et al., 2015; Fan et al., 2020). Given the limited
47 available time, a complete and reliable analysis of the risks, requiring in-depth study of the phenomenon, is not
48 achievable during the event and only rapid assessments for the dam stability are suitable. When the people to
49 evacuate are too many or the related risk is too high, engineering measures for the hazard reduction are attempted:
50 among these are for example modification of slope geometry, drainage, retaining structures and internal slope
51 reinforcement (Popescu and Sasahara, 2009; Schuster and Evans, 2011). Therefore, part of the effects from
52 landslide damming can be avoided or at least reduced thanks to mitigation and prevention measures (e.g., slopes
53 stabilization or re-profiling) if the most critical areas with the highest damming probability are known.
54 Consequently, planning and prevention tools, such as risk and susceptibility mapping, are essential to reduce the
55 costs of natural hazard and improve the efficiency of environmental management.

56 Reactivation of ancient landslides triggered during different climatic and environmental conditions may often
57 generate new mass movements (Casagli and Ermini, 1999; Canuti et al., 2004; Dikau and Schrott, 1999; Borgatti
58 and Soldati, 2010; Crozier, 2010). Landslides generated in the past are ~~now-often~~ dormant, with strength
59 parameters of the sliding surface close to the residual ones, and difficult to recognize because vegetation, erosion
60 and superficial alteration hide their morphology. Natural causes, such as earthquakes, river undercutting, rainfall,
61 and snowmelt, or even anthropic activity can reactivate these ancient phenomena. Therefore, all dormant landslides
62 capable to reach a river along their pathway can potentially dam it and should be investigated. New landslides,
63 instead, may develop wherever are present suitable conditions along the slopes. The spatial occurrence probability
64 is commonly assessed by landslide susceptibility analysis, highly dependent on landslide volume (Catani et al.,
65 2016), which is difficult to accurately predict.

66 Landslides in Central Asia are quite common and a considerable number of them have huge dimension, often
67 induced by strong earthquakes but also by floods, heavy rainfall and snowmelt (Behling et al., 2014; Golovko et
68 al., 2015; Havenith et al., 2015a; 2015b; 2006b; Kalmetieva et al., 2009; Rosi et al., 2023; Saponaro et al., 2014;

69 Strom and Abdrakhmatov, 2017; 2018). Concerning landslide dam events, in Central Asia regions several mass
70 movements of considerable size produced the obstruction of a river section, of which more than 100 still are
71 existing with a lake (Strom, 2010). Although many of these could be considered stable (Strom, 2010), the
72 occurrence of devastating outburst floods in the last century show that their potential hazard should never be
73 overlooked also considering the seismicity of the region. In the Rushan and Murgab districts of Gorno-Badakhshan
74 Autonomous Oblast (Pamirs, Tajikistan) along the Murghab river, the Usoi [landslide](#) dam is one of the most
75 famous of the many cases in the regions. Its impounded lake, called Lake Sarez, is 60 km long with 500 m of depth
76 and has a stored volume of about 17 km³, representing the world deepest landslide-dammed lake (Costa and
77 Schuster, 1991; Fan et al., 2020). It was originated on February 18th, 1911, when a MW 7.2 earthquake triggered
78 a giant wedge-failure of about 2.2 km³ of rock (mainly quartzite, schist, shale and dolomite) and debris that blocked
79 the Murgab River and a tributary valley, forming the 560 m high, 5 km long and 4 km wide Usoi dam, impounding
80 Lake Sarez, also creating the smaller Lake Shadau (Strom, 2010).

81 Landslide dam evolution, according to some studies (Swanson et al., 1986; Ermini and Casagli, 2003; Dal Sasso
82 et al., 2014; Tacconi Stefanelli et al., 2016), can be estimated through geomorphological indexes which require
83 parameters characterizing the landslide (or the dam) and the river (or the lake). Geomorphological indexes are a
84 powerful classification tool, but their prediction power depend mainly on long studies, a large amount of data and
85 measurement efforts given their empirical nature. Many of these indexes need parameters not always available and
86 easy to acquire, such as grain size distribution (Liao et al., 2022) or landslide velocity (Swanson et al., 1986).

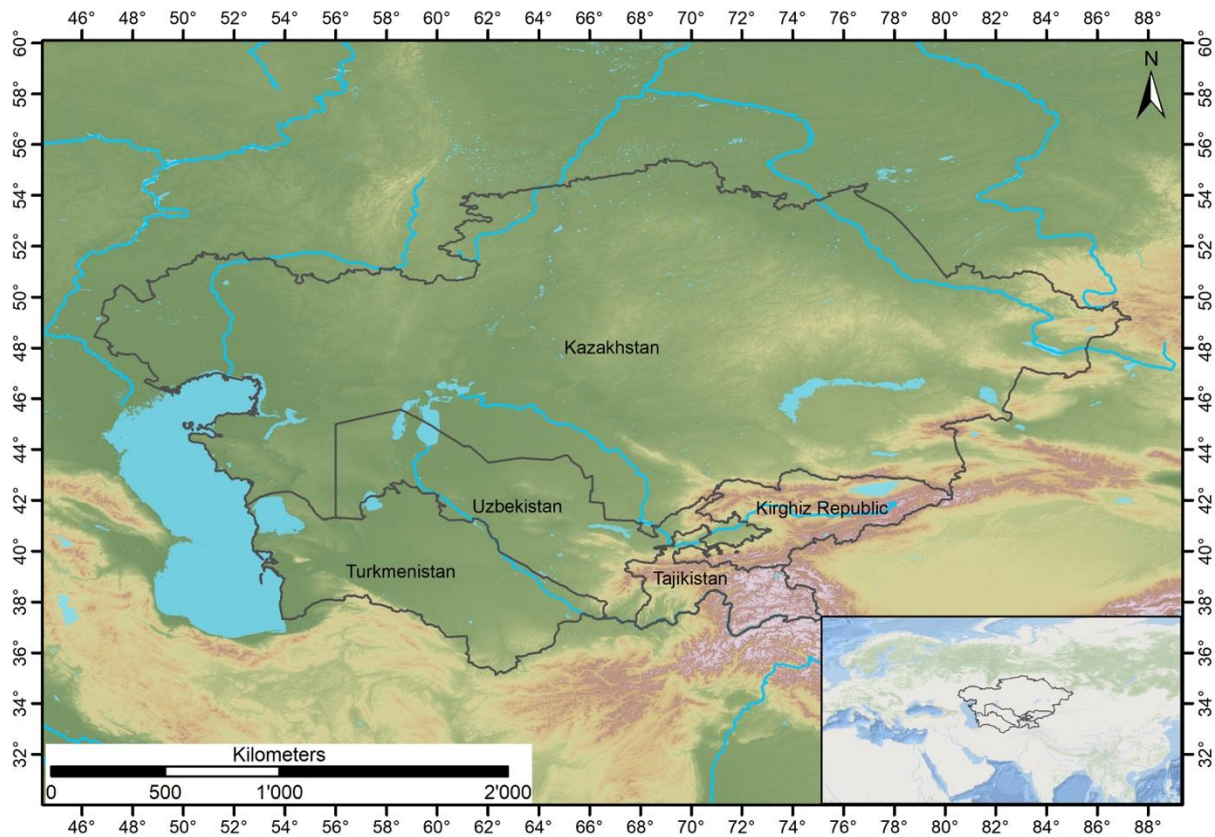
87 In this work, we propose a simple semi-automatic GIS-based mapping methodology to verify the damming
88 susceptibility of river networks at national scale from existing and neo-formed landslides trough a
89 geomorphological index. This activity research was carried out in the framework of the SFRARR Project
90 (*“Strengthening Financial Resilience and Accelerating Risk Reduction in Central Asia”*) as a part of a multi-hazard
91 approach ([Peresan Bazzuro](#) et al., 2023).

92 The proposed mapping methodology represents an innovation in terms of application simplicity, availability of
93 data and of extension of the analysed area, bringing new information on the damming hazard in the Central Asia
94 regions where the landslide susceptibility is quite high (Rosi et al., 2023) and a set of input data required for the
95 methodology application were available.

96 **2 Study area**

97 Central Asia is a region of vast diversity encompassing high mountain chains, deserts, and steppes (Figure 1). The
98 southern and eastern parts of the region are predominantly occupied by the mountainous areas of Djungaria, Tien
99 Shan, Pamir, Kopetdag, and a small part of Western Altaj, with peaks exceeding 7,000 m above sea level (a.s.l.)
100 (Strom, 2010). These intraplate mountain systems, developed in the Cenozoic as a result of the India-Asian
101 collision, is located between the Tarim Basin and the Kazakh Shield (Molnar and Tapponier 1975, Abdrakhmatov
102 et al., 1996; 2003; Zubovich et al., 2010; Ullah et al., 2015). This study focusses the attention on the territories
103 of Central Asia that includes Turkmenistan, Kazakhstan, Kyrgyz Republic, Uzbekistan, and Tajikistan, covering
104 a surface of more than 4·10⁶ km². Mountain building began in the Oligocene (Chedia, 1980) or later

105 (Abdrakhmatov et al., 1996), resulting in a complex system of basement folds interrupted by several thrusts and
106 reverse faults with lateral offset of important amounts (Delvaux et al., 2001).



107

108 **Figure 1. Geographical and geomorphological framework of the study area.** Lake's polygons from Esri,
109 Garmin International, Inc.; topographic base from NASA's SRTM project (Far and Kobrick, 2000).

110 The mountain belts contain several regional fault zones (Figure 2), and others cross the mountain systems with a
111 NW-SE axis (Trifonov et al., 1992). Paleozoic crystalline rocks form, for the most part, the mountain ridges which
112 correspond to a neotectonic anticline and are separated by tectonic depressions, with lenticular or linear shapes.
113 These intermountain depressions host the primary river valleys and are filled by Neogene and Quaternary deposits,
114 principally sandstones, siltstones interbedded by gypsum, and conglomerates (Strom and Abdrakhmatov, 2017).
115 Lithologies from Mesozoic and Paleogene are characteristic of the areas at the foot of mountain ranges (Figure 2).
116 This main deeply incised river network, fed by glaciers, snowmelt water and rain, is linked by narrow deep gorges
117 up to 1-2 km deep (Strom and Abdrakhmatov, 2018) and is the origin of most of the rivers in Central Asia.

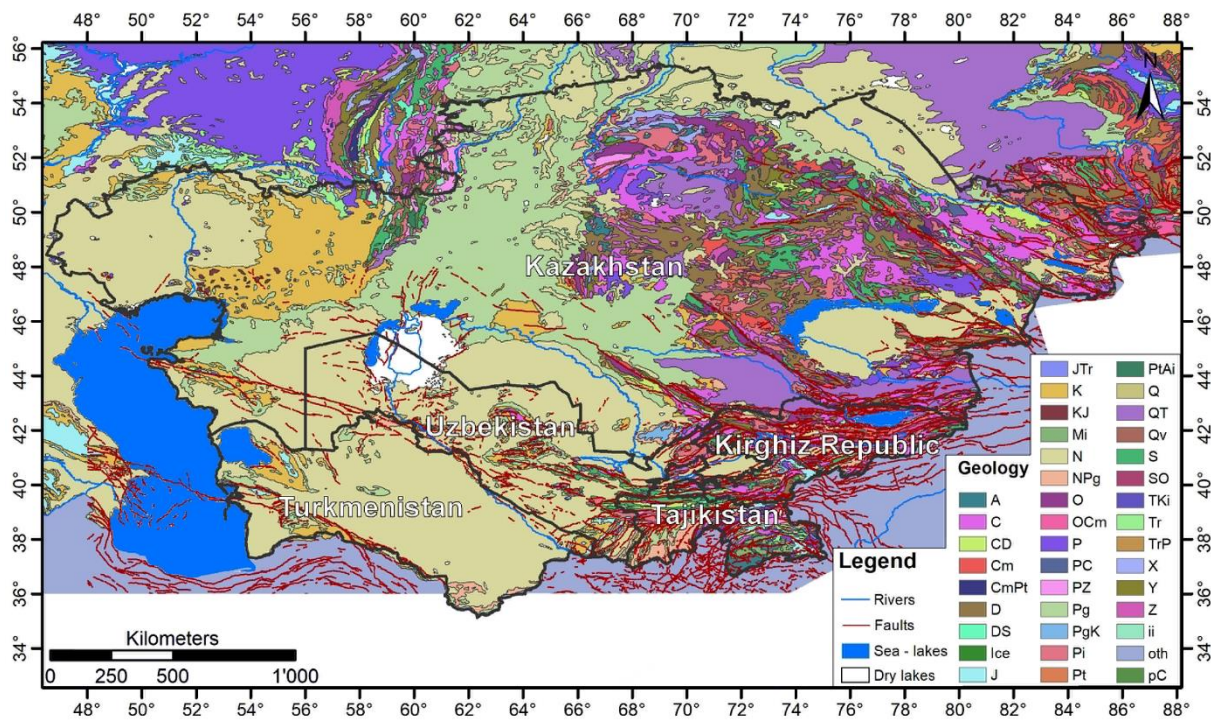


Figure 2. Geological map of the area. Geological formation data are from the United States Geological Survey (USGS) (Persits et al., 1997, for the legend), faults are from the Active Faults of Eurasia Database (AFEAD) (Styron and Pagani, 2020).

The retreat and shrinkage of glaciers in Central Asia regions induced by the global warming produce a seasonal variation in river discharge and consequently an increase of its induced hazards such as glacial-Glacial Lake outburst-Outburst Floods (GLOFs) (Falátková, 2016), resulting in countless losses of human life and destroyed infrastructure (Kropáček et al., 2021; Petrov et al., 2017; Wang et al., 2013). The high seismicity, frequent floods and a complex geological and topographical structure (such as lithological predisposition, faulting zones, steep slopes) contribute to predispose the region to frequent landslides which can potentially obstruct the narrow valleys of the mountain ranges and in turn be the cause of chain risks (CAC DRMI, 2009; Havenit et al., 2017).

3 Materials and Methods

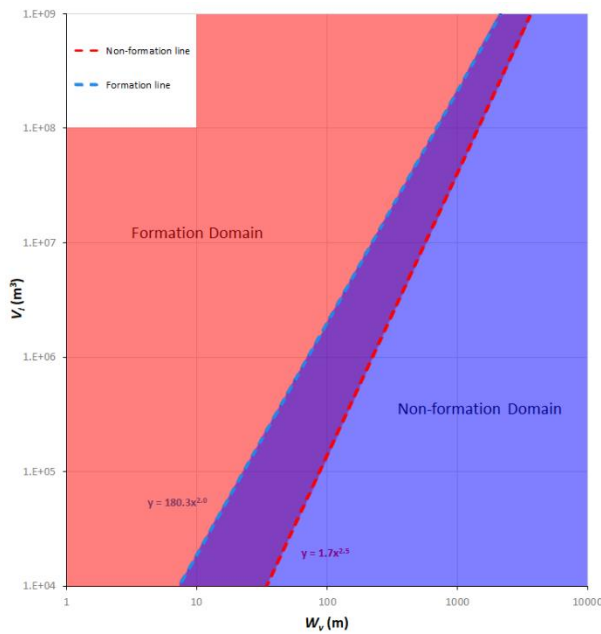
The Morphological Obstruction Index (MOI) (Tacconi Stefanelli et al., 2016) is a bivariate index able to evaluate the potential hazard posed by landslide dams that requires only simple morphometrical parameters which are easily extracted from common Digital Elevation Models. The MOI is based on the interpolation of 351 documented cases and has been used in several studies, such as in Italy and Peru (Tacconi Stefanelli et al., 2016; 2018), to assess landslide damming susceptibility showing better results than others popular indexes (Swanson et al., 1986). This empirical index ~~It is~~ is a useful tool for identifying high-risk areas and for prioritizing mitigation efforts in landslide-prone regions.

The MOI is calculated by dividing the volume of the landslide, V_l (m^3), by the width of the river valley, W_v (m), at the dam location.

$$MOI = \log \left(\frac{V_l}{W_v} \right) \quad (1)$$

The MOI is based on the principle that the higher the ratio of the landslide volume to the river width, the greater the potential for dam formation. It is important to point out that river width, W_v , shall be defined as the width of the river valley which can potentially be obstructed creating a dammed lake and not of just the channel where the river flows, as is often misinterpreted, although in narrow mountain valleys these often coincide.

Landslide dams analyzed by the index can be grouped within three evolutionary classes: formed (the red area, where the plotted landslides have completely blocked their river), not formed (the blue area, where only cases of unobstructed rivers are found) and of uncertain evolution (the purple area, in which both cases of formed and unformed dam can be found). The limits of these domains are depicted by two lines, the lower red “Non-formation line” and the upper blue “Formation line” (Figure 3Figure 3Figure-2) obtained by the interpolation of the cases analyzed by Tacconi Stefanelli et al. (2018).



150
151 **Figure 332. Schematic plot of the non-Formation line and Formation line.**

152 The equation of the former is expressed as follows:

$$V_l' = 1.7 \cdot W_v^{2.5} \quad (2)$$

154 Where V_l' is the “Non-formation volume” and is the minimum landslide volume able to potentially block a river
155 with a given width W_v . Smaller volumes cannot completely dam the river. The latter expression draws the upper
156 limit for not formed dams and is expressed as follows:

$$V_l'' = 180.3 \cdot W_v^2 \quad (3)$$

158 Where V_l'' is the “Formation volume”, is the minimum landslide volume able to dam the river valley, with a
159 confidence of 99%, and the inferior boundary of the Formation domain (which includes only formed dams).

160 Intermediate cases that fall between the two lines cannot be confidently identified as formed or unformed and are
161 therefore classified as having uncertain evolution.

162 As originally proposed by Tacconi Stefanelli et al. (2020), these two equations, Eq.(2) and (3), can be used to
163 apply a simple semi-automatic methodology in order to verify at basin scale the damming susceptibility from
164 existing and neo-formed landslides. The following semi-automated procedure, inspired by the one of Tacconi
165 Stefanelli et al. (2020) of which this represents an improvement, is applied on a national scale and can be
166 reproduced entirely in a GIS (Geographic Information System) environment. However, the method, being initially
167 designed for analysis at basin/region scale, applied to such a small scale (national) will not be able to provide
168 detailed information. For this reason, this study represents a preliminary phase of investigation which will allow
169 to concentrate further detailed analysis on the areas identified as more critical.

170 Within an even medium-long time interval the valley width in each river stretch does not change significantly and
171 can be considered an immutable factor in the MOI equation (Eq.(1)). Starting from this assumption, along with
172 Eq. (2) and Eq. (3), if the average river width W_v of each river stretch can be assessed, the two threshold landslide
173 volumes V_1' (Non-formation volume) and V_1'' (Formation volume) can be estimated for each river stretch.

174 Landslides that cause river obstruction are in many cases reactivations of ancient movements that are still in a
175 condition of partial instability and that have not reached a potential equilibrium reaching the valley floor.
176 Therefore, with a landslide inventory it is possible to assess, with some assumptions and simplifications, which
177 among the mapped landslides are able to dam the river section. Each landslide that is not already laying in the
178 valley floor with a volume bigger than V' and V'' are identified as potentially prone to block the river in the future
179 in that point. Then, a "Map of Damming Susceptibility" for reactivation of existing landslides can be generated.

180 The likelihood prediction for new landslides, with volume bigger than V_1' and V_1'' , is a much more difficult task
181 as the volume is a complex value to be estimated (Catani et al., 2016). The exceeding probability of landslide
182 volume used by Tacconi Stefanelli et al. (2020) was reached thanks to the knowledge of the alpha exponent of the
183 statistical frequency distribution of the landslide volumes in the whole study area. To achieve this, a database of
184 landslides with a very high number of events (tens or even hundreds of thousands) should be available (Catani et
185 al., 2016), which in our study area unfortunately is not. To have an assessment of the damming susceptibility for
186 neo-formed landslides the two volume threshold values, evaluated for all the river networks, can be used as well.
187 After estimating the river width of every river stretches, the V_1' and V_1'' values of each of them can be computed
188 through the corresponding two equations. In this way there will be two reference values to be able to assess whether
189 the volume of a new landslide can potentially obstruct an affected river stretch.

190 The input data needed for the procedure are a Digital Elevation Model, a vector layer of the river network, and an
191 updated landslide inventory. The data quality and resolution such as the landslides inventory completeness, the
192 river network reliability and the DEM's pixel size heavily affect the quality of the result (Tacconi Stefanelli et al.,
193 2020). Thus, it was decided to use the DEM with the higher resolution freely available from the NASA's SRTM
194 project (Far and Kobrick, 2000) with a 1 arc-second, or about 30 meters of resolution. The river network came
195 from Coccia et al. (2023). The latter input data is a database of 8910 landslides, that is a compilation of several

196 different inventories collected through decades of field surveys, studies and remote sensing analysis in the study
197 area, shown in [Figure 4](#)~~Figure 4~~[Figure 3](#).

198 Hereafter the detail of each inventory:

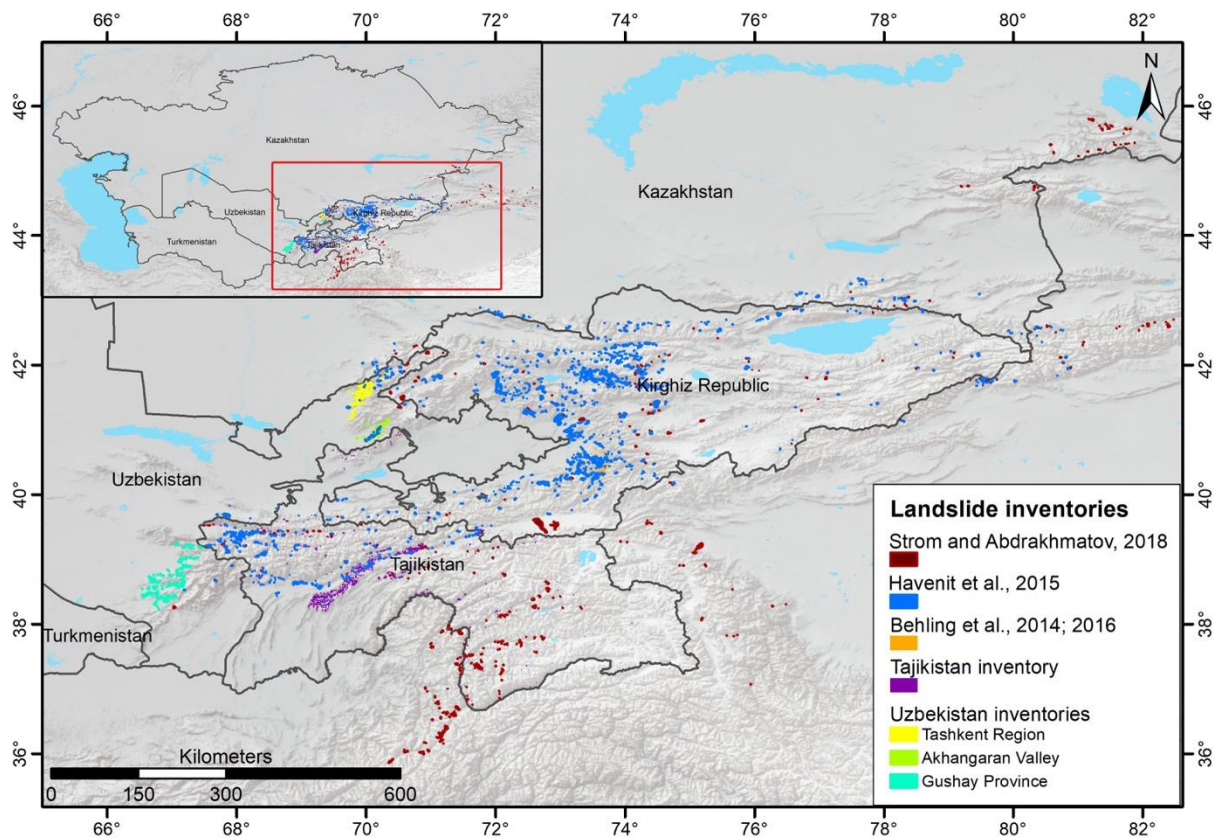
199 • The “Rockslides and Rock Avalanches of Central Asia” (Strom and Abdrakhmatov, 2018): an inventory
200 including more than 1000 of very big ($\geq 1 \text{ Mm}^3$) rockslides and rock avalanches, covering central Asian countries
201 (excluding Turkmenistan and Altai) and also Chinese Tien Shan and Pamir, and Afghan Badakhshan. Collected
202 in decades of field survey and analysis of aerial/satellite imaging, it includes also information on morphometric
203 parameters (runout, area), dammed lakes, head-scarps, and quantitative characteristics (such as area, volume) for
204 about 600 cases.

205 • The “Tien Shan landslide inventory” (Havenith et al., 2015a): is the biggest database in the study area.
206 Assembled through field work, remote sensing and geophysical data interpretation, it includes the elements of the
207 previous inventory alongside other smaller landslides in soft sediments (Havenith et al. 2006a; Schlögel et al.,
208 2011) for a total of 3,462 landslides polygons, including information on landslide length and area.

209 • The “Multi-temporal landslide inventory for a study area in Southern Kyrgyz Republic derived from
210 RapidEye satellite time series data (2009 – 2013)” (Behling et al., 2014; 2016; [Behling and Roessner 2020](#)),
211 includes 1,582 landslide polygons mapped from multi-sensor optical satellite time series data (from 1986 to 2013)
212 over an area of 2,500 km² in the Fergana valley rim in southern Kyrgyz Republic, and include information on
213 landslide activity (area and year of trigger).

214 • The “Tajikistan landslide database” produced by the Institute of Water Problems, Hydropower,
215 Engineering and Ecology of Tajikistan (IWPHE), with 2,710 landslide polygons and 114 landslide-prone areas,
216 including information on landslides length and area.

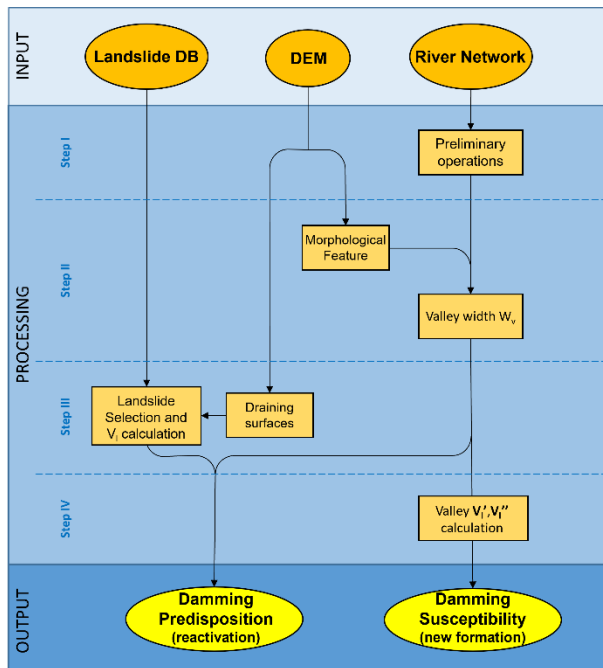
217 • The Institute of Seismology of the Academy of Science of Uzbekistan (ISASUZ) provided an inventory
218 which covers the Tashkent province composed by a point inventory ([Niyazov, R.A. 2020](#)) and a polygon inventory
219 (345 landslide) digitized from the maps in Juliev et al., 2017.



220

221 **Figure 443. Map of the landslide inventories in the study area.** Lake's polygons from Esri, Garmin
 222 International, Inc.; basemap from Esri, USGS, NOAA.

223 The methodology adopted to obtain the maps of damming susceptibility, derived from Tacconi Stefanelli et al.
 224 (2020), is summarized in the following main steps displayed in [Figure 5Figure 5Figure 4](#). According to the
 225 literature (Swanson et al., 1986; Fan et al., 2014; 2020; 2021; Tacconi Stefanelli et al., 2015; 2018), river
 226 obstructions occur in most of the time within hilly or mountainous areas and specially along steep slopes.
 227 Therefore, considering the extension of the study area, in order to reduce the time of elaboration and improve the
 228 visualization of the results, in step I of [Figure 5Figure 5Figure 4](#) a series of unnecessary data were removed from
 229 the calculations during some preliminary operations. For this reason, river that flow in flat areas (with less than
 230 4° slopes) were not considered in the elaborations, since their damming probability is certainly very low with an
 231 extremely wide valley width, and the potential impounded lake should have a negligible volume. Additionally, to
 232 have maps easier to manage and display, the river network was split in 5 km long river stretches consecutive to
 233 each other.

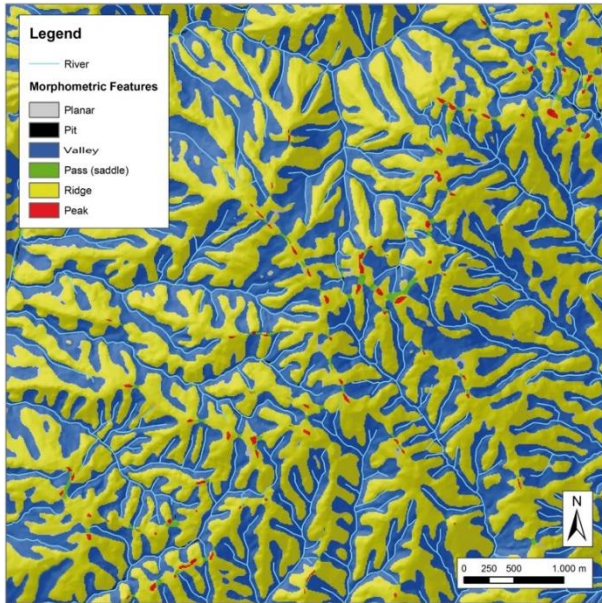


234

235 **Figure 554. Flow chart of the main steps of the mapping methodology.**

236 In applied geomorphology and natural science studies the analysis and characterization of the landscape has
 237 evolved during the last decades with the increasing accessibility of remote sensing data and the development of
 238 different algorithms able to automatically extract morphological features and landform information even at broad
 239 scales (Drăguț and Dornik, 2016; Maxwell and Shobe, 2022; Righini and Surian, 2018; Wang et al., 2010).

240 As already mentioned, the clear definition of the width of a river can be subjective and its measurement difficult
 241 to repeat especially if performed by different operators. In step II of [Figure 5](#)~~Figure 5~~~~Figure 4~~, an objective
 242 automatic method to extract morphometrical parameters have been chosen also for this reason. Wood (2009)
 243 implemented the “*LandSerp*” software (already incorporated in SAGA GIS or QGIS software), designed to
 244 automatically classify landforms from DEMs. Similarly for pattern detection and texture analysis within image
 245 processing, the software extracts land-surface parameters (e.g., slope, aspect, and curvature) from DEMs through
 246 a multi-scale approach. During these processing, the algorithm performs a classification of the landscape, grouping
 247 the landforms with homogeneous morphometric characteristics (pits, channels, peaks, ridges, passes, and planes)
 248 as shown in [Figure 6](#)~~Figure 6~~~~Figure 5~~. Thanks to this algorithm of morphological forms analysis proposed by
 249 Wood (2009), the polygons representing the morphological unit of the river valley can be automatically defined
 250 objectively even in a large area and extracted.



251

252 **Figure 665. Classification of the landscape into morphological classes according to Wood (2009) (modified**
 253 **from Tacconi Stefanelli et al., 2020).**

254 The effectiveness of distinguishing different morphological landforms of this automatic tool is greater in
 255 mountainous regions characterized by significant differences in elevation, compared to flat areas where
 256 distinctions between landforms are less evident. The accuracy of the output is directly correlated with the resolution
 257 of the DEM, which should ideally be about a few meters. Coarser resolutions result in landslide volumes with a
 258 corresponding level of uncertainty.

259 The following phase is to provide to each river stretch a value of a valley width, W_v . A series of 1 km long lines
 260 (hereafter “transects”) are generated, perpendicular to the stretches of the river network, outdistanced by 500
 261 meters apart from each other. The created river valley polygons are used to “cut” the transects and then to measure
 262 the distance between the two river valley borders through the length of the cut transects.

263 Next, the valley widths (W_v) for each segment of the river are determined by assigning them an average value
 264 based on N perpendicular transects, excluding the extreme values (maximum and minimum, respectively W_{max}
 265 and W_{min}), as in the following equation:

$$266 \quad W_v = (\sum_{i=1}^n W_i - W_{min} - W_{max}) \frac{1}{n-2} \quad (4)$$

267 By utilizing an updated database of landslide polygons, in the step III of ~~Figure 5~~~~Figure 5~~~~Figure 4~~ it is possible to
 268 determine if a reactivated landslide is big enough to cause a complete river blockage thanks to the comparison
 269 with the boundary volumes of V_1' (below which a landslide cannot completely block the river) and V_1'' (above
 270 which the river valley is dammed for sure). A reactivated landslide should follow a downhill path akin to the flow
 271 of surface water. Within each slope, the drainage directions can be easily determined along the river network using
 272 a GIS software. Each mass movement can then be linked to the corresponding river stretch it would reach if
 273 reactivated based on their corresponding draining surfaces.

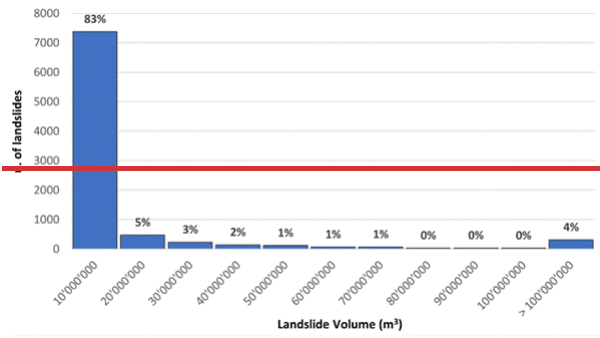
274 Since the information provided by the available inventories in the study area are not homogeneous and comparable,
275 for the computation of the landslide volume were chose to use the areas of the landslide polygons, since it is the
276 most common data. An experimental statistical relationship between areas and volumes was applied:

$$277 V_l = \varepsilon \cdot A_l^\alpha \quad (5)$$

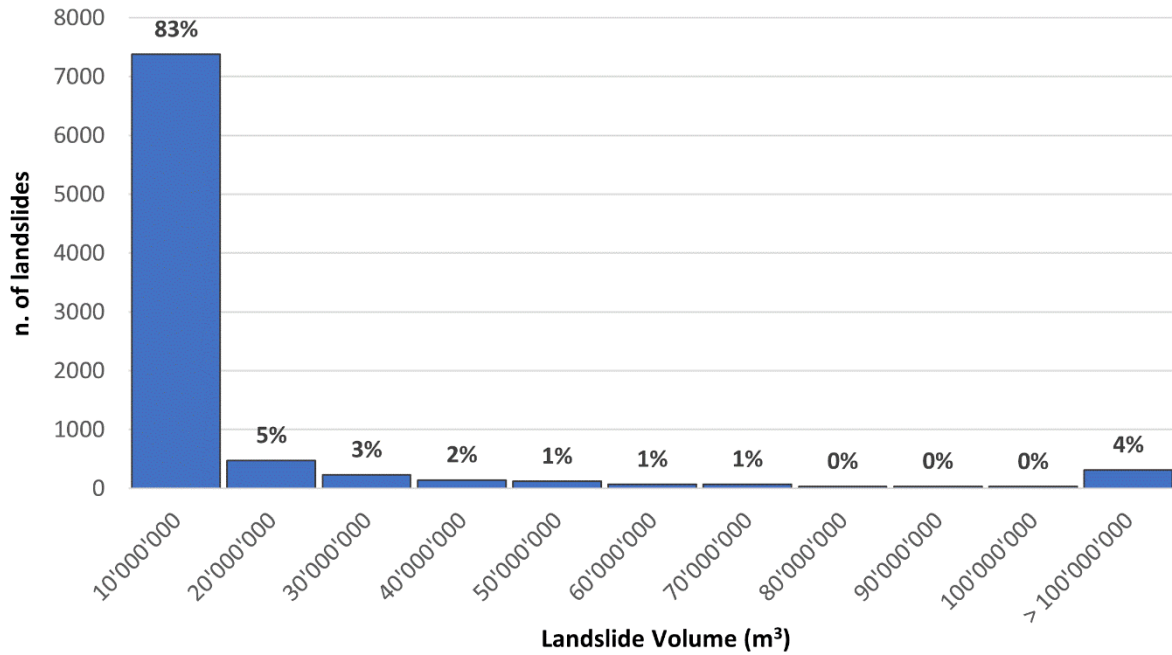
278 where V_l and A_l are respectively the volume and the area of a landslide, ε and α are respectively the constant and
279 the exponent of the power law describing the landslides volumes frequency distribution. Various experimental
280 relations of ε and α have been employed for landslide volume calculations by researchers located in different
281 countries. After an evaluation of these relations in the study area, the parameter proposed by Guzzetti et al. (2009)
282 have been selected because of the number of the studied cases (667) and the magnitude range of the landslides
283 area investigated (from 10^1 to 10^9 m²). The landslide volume computed using this procedure is based on some
284 approximations, since they use geometric simplifications, but it does still reflect the magnitude of the process. The
285 result of the computation in ~~Figure 7~~~~Figure 7~~~~Figure 6~~ shows an almost bimodal distribution, in which most
286 landslides (83%) have moderate volumes, lower than 10 million m³ (with 63% lower than 1 million m³), but 4%
287 have value higher than 100 million m³.

288 Then, ~~Table 1~~~~Table 1~~~~Table 1~~ is used to assign to each landslide of the inventory a classification based on the
289 comparison with the boundary volumes V_l' and V_l'' , with value of 2 if the calculated landslide volume, V_l , is
290 bigger than V_l' (or V_l''), of 0 if it is smaller. For more caution, the V_l values is increased by an arbitrary value of
291 20% ($V_l \cdot 1.2$) to avoid any potential underestimation during volume estimation and even the possible increase of
292 landslide size with the reactivation due to the mechanism of material entrainment (Hungr ~~&~~~~and~~ Evans, 2004). For
293 each landslide, if the computed boundary volume V_l' (or V_l'') is bigger than the estimated landslide volume V_l ,
294 but smaller than $V_l \cdot 1.2$, then a classification value of 1 is attributed.

295 The damming susceptibility of each mapped landslide is assigned by integrating the two comparative classification
296 values from the intensity matrix illustrated in ~~Figure 8~~~~Figure 8~~~~Figure 7~~. The matrix establishes five qualitative
297 classes on a scale of severity for damming susceptibility, ranging from Very Low (dark green) to Low (light green),
298 Moderate (yellow), High (orange), and Very High (red). The combination of a high V_l'' value (1 or 2) and a lower
299 V_l' value (0 or 1) symbolized by gray squares is not possible according to their respective formulations.



300



301

302 **Figure 776.** Landslide volumes frequency distribution in the central Asia regions.

303 **Table 1.** Comparison table between landslide calculated volumes, V_l , with the boundary volume of Non-
 304 formation and Formation, V_l' and V_l'' (after Tacconi Stefanelli et al., 2020).

	$V_l > V_l' (V_l'')$	$V_l < V_l' (V_l'') < V_l * 1.2$	$V_l < V_l' (V_l'')$
Classification Value	2	1	0

305

V_i' \ V_i''	0	1	2
0	Very Low		
1	Low	Moderate	
2	Moderate	High	Very High

306

307 **Figure 887. Predisposition matrix used for the assignment of the damming predisposition intensity to the**
 308 **mapped landslides (after Tacconi Stefanelli et al., 2020).**

309 Even if the proposed method is objective, it is certainly not free from uncertainties and errors. The 20% increase
 310 applied to mapped landslide volumes to reduce underestimation errors can in turn produce false positives for
 311 overestimation errors. While a false positive is preferable to a false negative (according to a principle of prudence),
 312 too many high-risk false positive cases "spread" an unreal risk throughout the area instead of concentrating it in
 313 sites of real risk. Therefore, it can be assumed that the landslide bodies which have previously reached the valley
 314 floor have already generated most of their effect on the river network (Strom, 2010) or have had no effect, spending
 315 their potential risk component. These landslides, also with a volume higher than V_i' and V_i'' and therefore classified
 316 with Very High dam predisposition, even if reactivated probably will not produce any further effect in the future.
 317 For these reasons, it was decided to downgrade the classification of those landslides that intersect the river network
 318 by reducing its position of the classification of damming predisposition by one class.

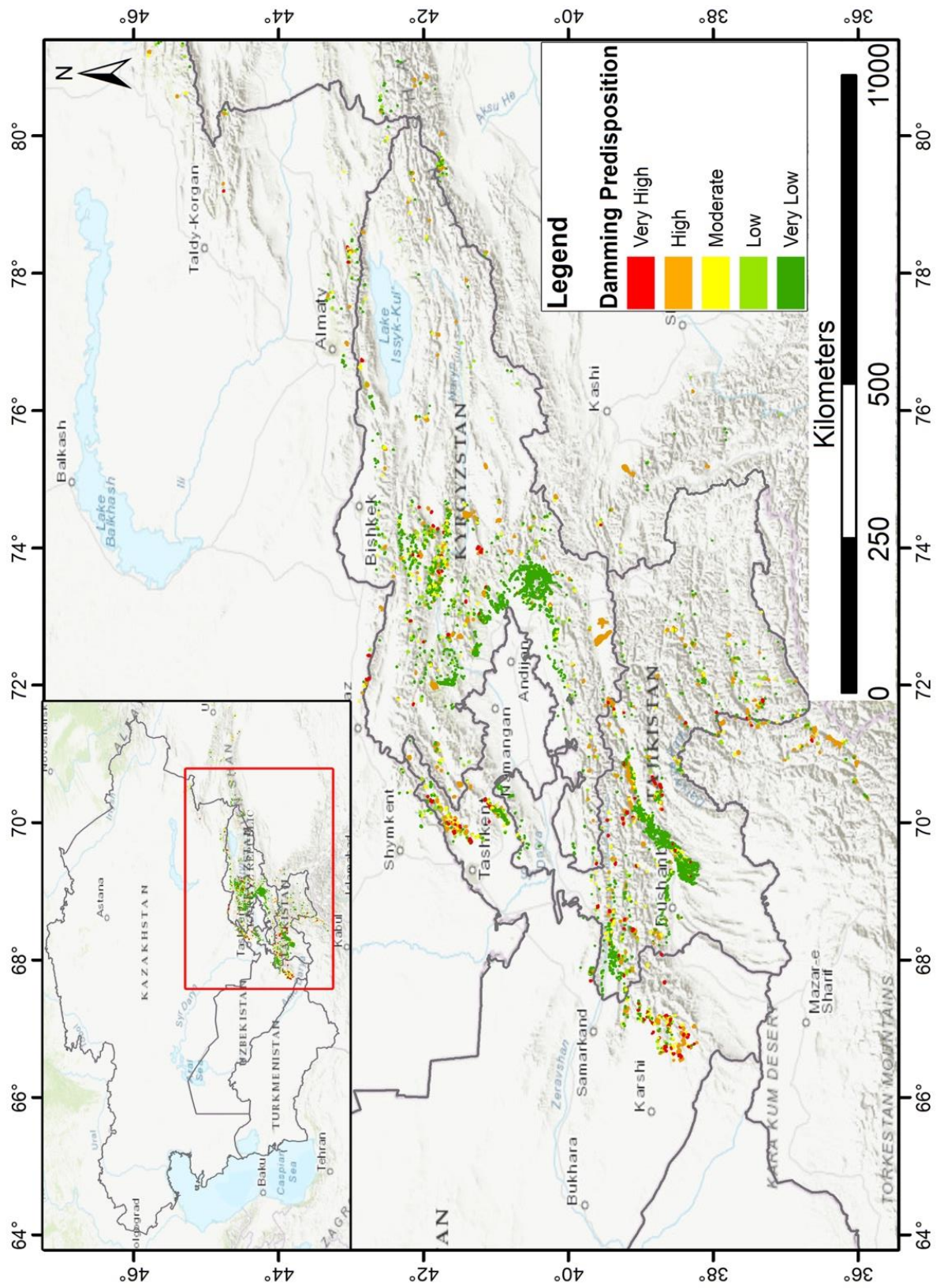
319 Using the W_v value for each river stretches estimated during the step III of [Figure 5](#)~~Figure 5~~[Figure 4](#), in the last
 320 step (IV) the two boundary landslide volumes, namely "Non-formation volume" and "Formation volume" (V_i' and
 321 V_i''), can be estimated by applying the equations of the "Non-formation" (Eq. (2)) and "Formation" lines (Eq. (3)).
 322 These two values can be used both to classify the damming susceptibility of the river network (for new landslides)
 323 and of the landslides inventory (for their reactivation). For the first case, the computed volume values V_i' and V_i''
 324 embody the required volumes of a new landslide to have a potential or certain (with 99% of confidence) obstruction
 325 for each river stretches.

326 4 Results

327 The mapping methodology was applied to all the studied territories of the Central Asia region in order to analyze
 328 and evaluate the results. Two smaller basins, the upper Pskem river and the Fergana valley, were selected to verify
 329 the reliability at a catchment scale of the results obtained from a methodology applied on a national scale. The

330 assessment of damming predisposition on the available landslide inventory on the Central Asia regions is shown
331 in the map of ~~Figure 9~~~~Figure 8~~, while a closer detail is reported in ~~Figure 11~~~~Figure 10~~ showing
332 the Kyrgyz Republic territory. The number of landslides (644 cases) classified with Very High damming
333 predisposition from the whole inventory before the class reduction due to the river intersection was unjustifiably
334 and unreasonably large posing excessive concern and risk perception. After the change, this number decreased by
335 75% up to 166 cases, a high number but more reasonable concerning such a large area. In the class distribution of
336 the damming predisposition shown in ~~Figure 10~~~~Figure 9~~ the most frequent class is the Very Low, with
337 81% of the whole database, followed by the Low and High classes both with 6% and the remaining percentage
338 divided among Moderate (5%) and Very High (2%).

339 This distribution is quite coherent with the landslide volumes frequency distribution since it is reasonable to
340 associate landslides with very low volume (83%, shown in ~~Figure 7~~~~Figure 6~~) with those classified with
341 very low susceptibility (81%, ~~Figure 10~~~~Figure 9~~). The landslides classified with the higher values of
342 susceptibility (Moderate, High, and Very High with a total of 13%) instead do not only include landslides with
343 higher volumes (more than 100 million m³ representing 4% of the total), meaning that also even smaller landslides
344 can potentially block narrow river stretches in these regions.



345

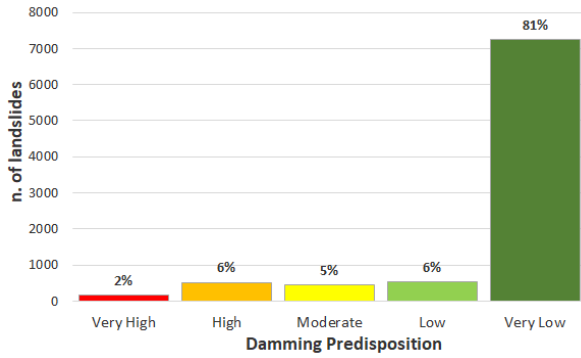
346

347

Figure 998. Map of Central Asia Landslide Damming Susceptibility. Basemap source: Esri, HERE, Garmin Intermap, increment P Corp, GEBCO, USGS, FAO, NPS, NRCAN, GeoBase, IGN, Kadaster NL, Ordnance

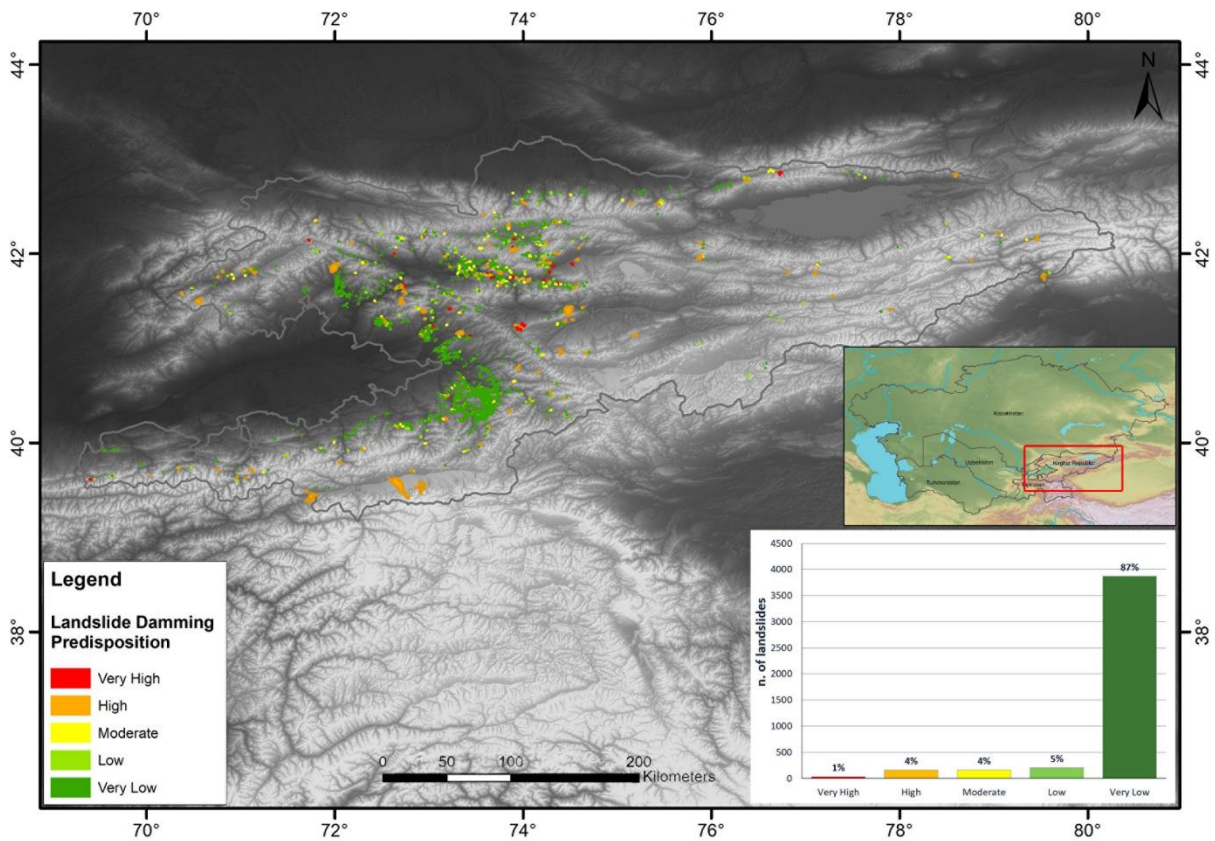
348 Survey, Esri Japan, METI, Esri China (Honk Kong), © OpenStreetMap contributors, and the GIS User
349 Community.

350



351

352 **Figure 10109. Classes distribution of the damming predisposition for landslides reactivation.**



353

354 **Figure 11110. Map of Damming Predisposition by landslides reactivation in Kyrgyz Republic territory.**

355 Topographic base from NASA's SRTM project (Far and Kobrick, 2000).

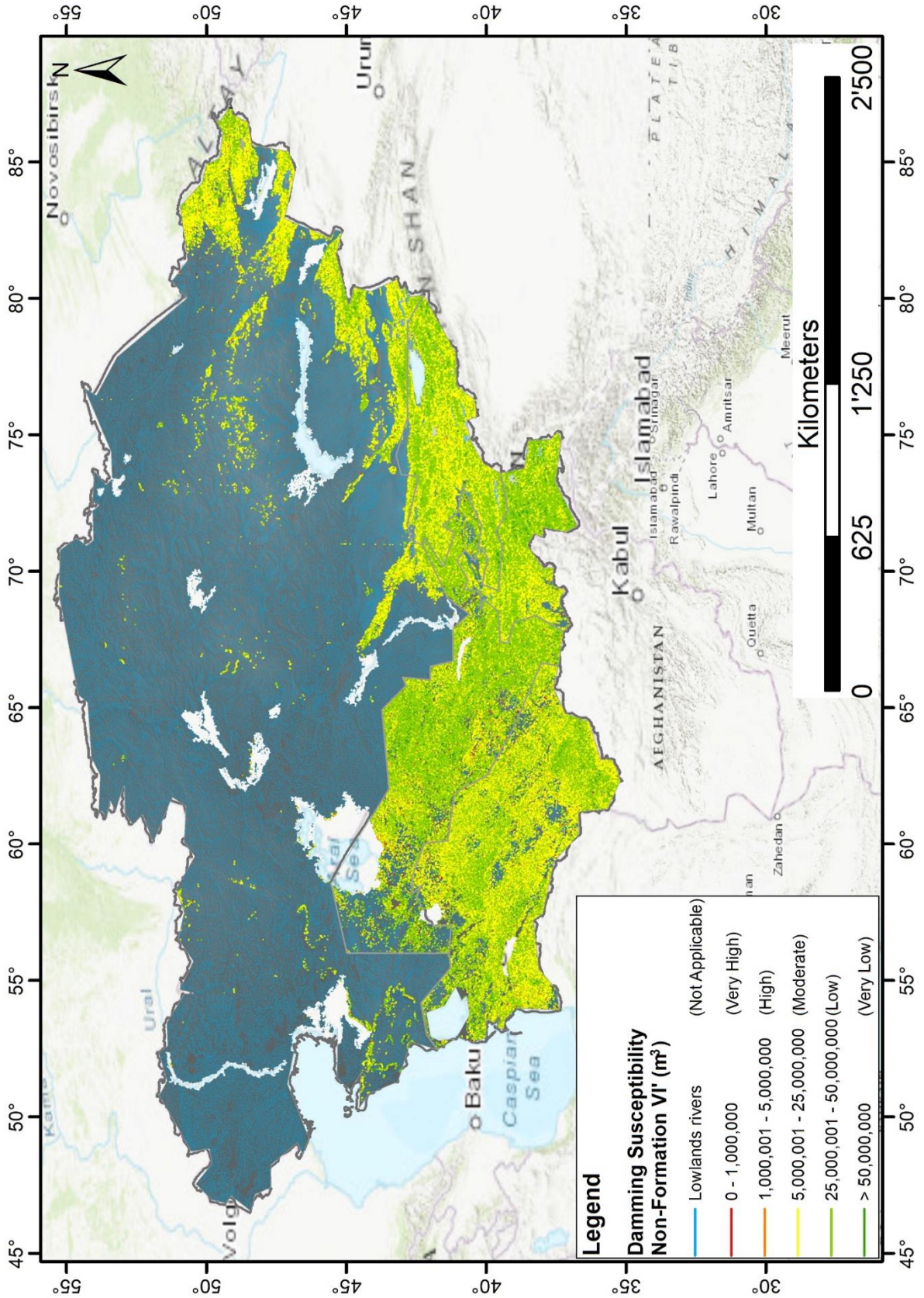
356 Concerning the damming susceptibility caused by new landslides along all the river network in the study area, two
357 different maps of the river networks have been produced using the Non-formation and Formation volumes values.
358 Although counterintuitive at first glance, these maps provide complementary information. The former provides
359 the volumes of landslides that surely create an obstruction, while the latter the volumes below which it definitely

360 does not form. According to the preliminary steps of the described methodology, in the river stretches running in
361 flat areas (slope degree less than 4° representing the 88.4% of the entire river network) the analysis has been not
362 applied, due to the extreme unlikelihood that a complete obstruction will occur in such areas. The magnitude of
363 the damming susceptibility of the river networks has been classified in five classes and shown in [Figure 12](#)[Figure](#)
364 [12](#)[Figure 11](#) and [Figure 15](#)[Figure 15](#)[Figure 14](#). The five volumes intervals describing damming susceptibility were
365 decided according to general value distribution of landslides volumes and an expert judgement. Since small
366 landslides are more frequent than large ones, as reported in [Figure 7](#)[Figure 7](#)[Figure 6](#), the lower is the landslide
367 volume required to realize an obstruction, the higher is the magnitude. In the map of damming susceptibility related
368 to the “Non formation”, reported in [Figure 12](#)[Figure 12](#)[Figure 11](#), the central classes, Moderate and Low are the
369 most frequent with 4.4% and 5.8% respectively, as reported in [Figure 13](#)[Figure 13](#)[Figure 12](#). This means that in
370 most of the river stretches in the study area the minimum landslide volume able to potentially dam the riverbed is
371 between the limit values of the two classes, from 2,5 to 25 million m³. The following most frequent class is the
372 Very Low with 0.8% and only a very small portion of the river stretches are classified as High and Very High with
373 just 0.4% and 0.2% with a required landslide volume less than 2.5 million m³. An example of close-up on the
374 Tajikistan territory is reported in [Figure 14](#)[Figure 14](#)[Figure 13](#).

375 Regarding the map of damming susceptibility related to Formation values, the map in [Figure 15](#)[Figure 15](#)[Figure](#)
376 [14](#) shows slightly different results. The most frequent classes are the two lower ones, Low and Very Low with
377 4.4% and 6% respectively, as described in [Figure 16](#)[Figure 16](#)[Figure 15](#). Only just the 0.3% and 0.4% fall in the
378 classes Very High and High damming susceptibility. A close-up on the Kyrgyz Republic is reported in [Figure](#)
379 [17](#)[Figure 17](#)[Figure 16](#).

380 The results of the classification for the river networks of each state are shown in [Figure 18](#)[Figure 18](#)[Figure 17](#) to
381 [Figure 22](#)[Figure 22](#)[Figure 21](#). The landslides of Tajikistan, Kyrgyz Republic, Uzbekistan and Kazakhstan regions
382 have been classified according to damming predisposition ([Figure 18](#)[Figure 18](#)[Figure 17](#)-a., [Figure 19](#)[Figure](#)
383 [19](#)[Figure 18](#)-a., [Figure 20](#)[Figure 20](#)[Figure 19](#)-a. and [Figure 21](#)[Figure 21](#)[Figure 20](#)-a). In the Turkmenistan territory,
384 it was not possible to assess any damming predisposition by landslides reactivation since the absence of any
385 available landslide inventory. The results of Uzbekistan and Kazakhstan regions ([Figure 20](#)[Figure 20](#)[Figure 19](#)-a.
386 and [Figure 21](#)[Figure 21](#)[Figure 20](#)-a.) are a bit different from Kyrgyz Republic and Tajikistan regions due to the
387 different availability of landslide inventories and a different ~~reliefs~~-orographic ~~structure~~-and valleys morphology
388 of the formers national territories. As already mentioned, for a clearer comprehension of the damming
389 susceptibility classification of the river network at the national level, the river stretches flowing in lowlands have
390 not been considered in the analysis. Concerning the Damming Susceptibility of Non-Formation ([Figure 18](#)[Figure](#)
391 [18](#)[Figure 17](#)-b., [Figure 19](#)[Figure 19](#)[Figure 18](#)-b., [Figure 20](#)[Figure 20](#)[Figure 19](#)-b., [Figure 21](#)[Figure 21](#)[Figure 20](#)-b.
392 and [Figure 22](#)[Figure 22](#)[Figure 21](#)-a.), the most frequent are Low and Moderate classes, followed by Very Low
393 class. Fortunately, only very few river stretches have been classified as Very High and High. For the Damming
394 Susceptibility of Formation ([Figure 18](#)[Figure 18](#)[Figure 17](#)-c., [Figure 19](#)[Figure 19](#)[Figure 18](#)-c., [Figure 20](#)[Figure](#)
395 [20](#)[Figure 19](#)-c., [Figure 21](#)[Figure 21](#)[Figure 20](#)-c. and [Figure 22](#)[Figure 22](#)[Figure 21](#)-b.) most of the rivers fall into
396 Very Low and Low classes, followed by Moderate class. Also in this case, only very few river stretches have been
397 classified as Very High and High. The results of the Tajikistan territory are quite similar to the Kyrgyz Republic

398 and Uzbekistan with which it shares a similar orographic distribution and morphology of the territory.
399 Turkmenistan and Kazakhstan show a slightly different distribution with higher percentage on Moderate class in
400 the Damming Susceptibility of Non-Formation and Low class in the damming susceptibility of Formation.



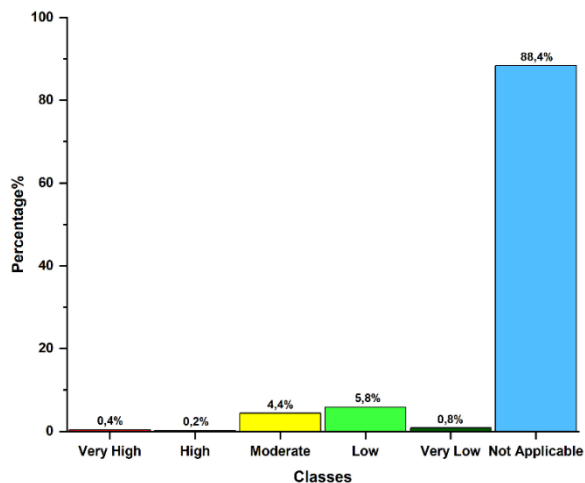
401

402

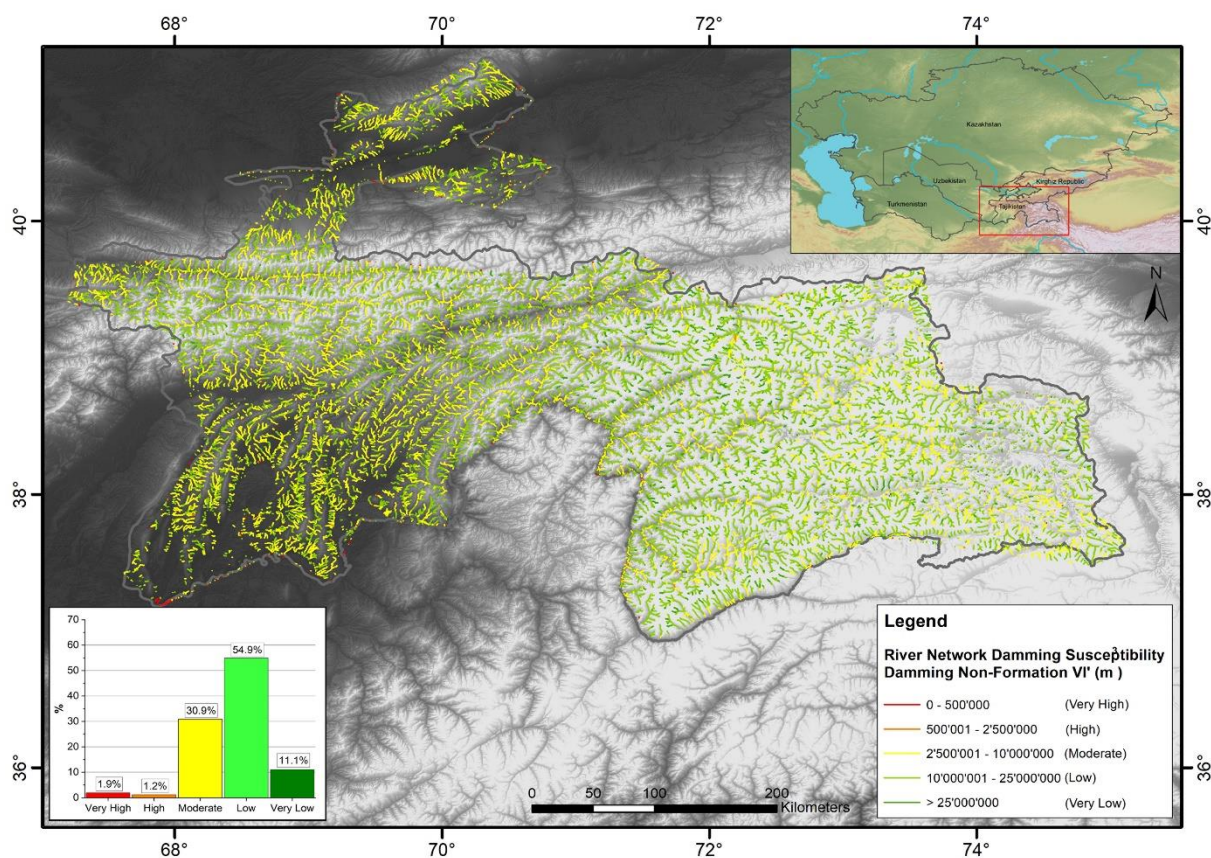
403

Figure 121211. Damming susceptibility map of non-formation of river stretches by new landslides in the region. River network database from Coccia et al., ([in prep. 2023](#)). Basemap source: Esri, HERE, Garmin

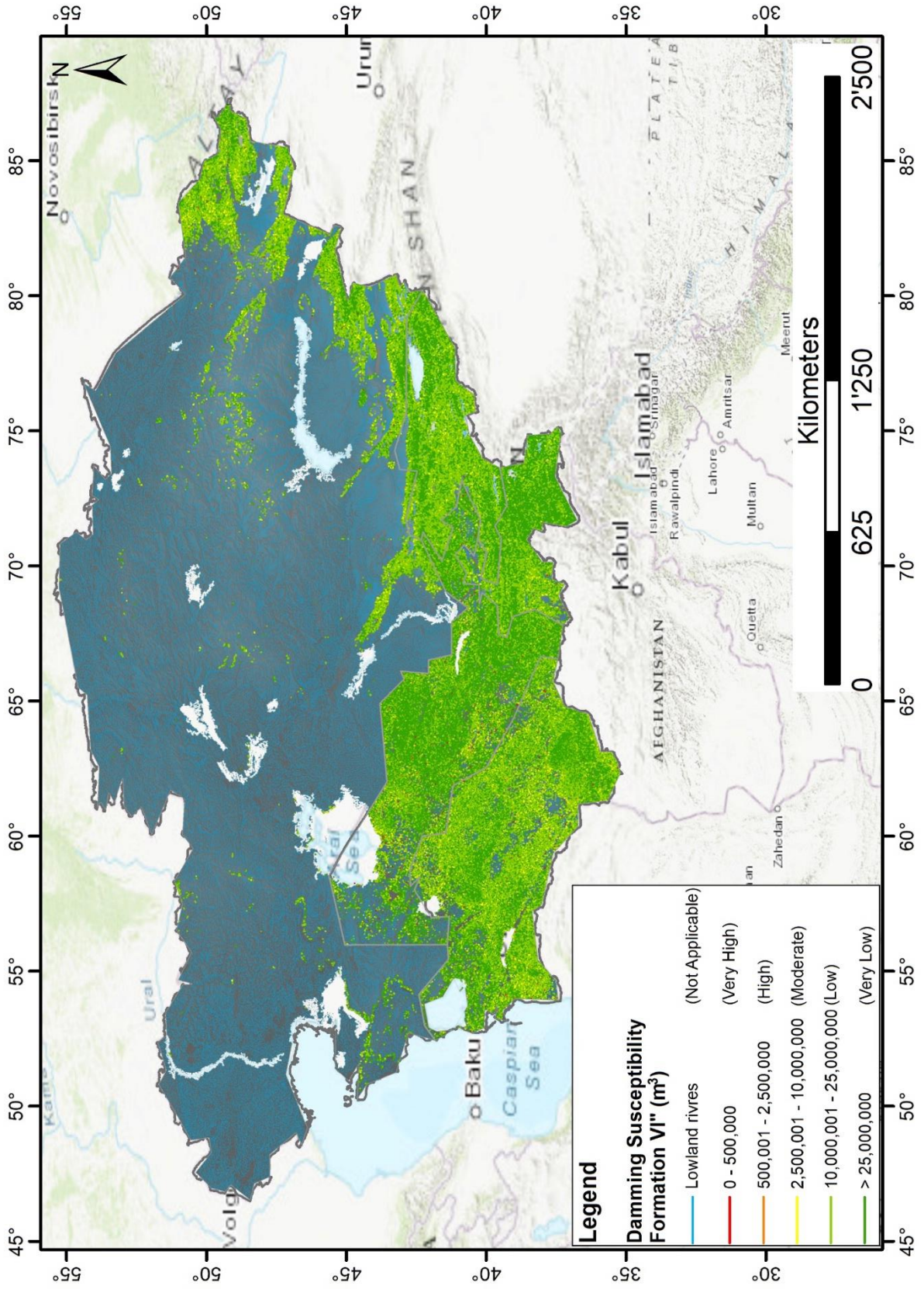
404 Intermap, increment P Corp, GEBCO, USGS, FAO, NPS, NRCAN, GeoBase, IGN, Kadaster NL, Ordnance
 405 Survey, Esri Japan, METI, Esri China (Honk Kong), © OpenStreetMap contributors, and the GIS User
 406 Community.



407
 408 **Figure 131312.** Distribution of the damming susceptibility in the study area by new landslides related to
 409 **Non formation boundary values.**



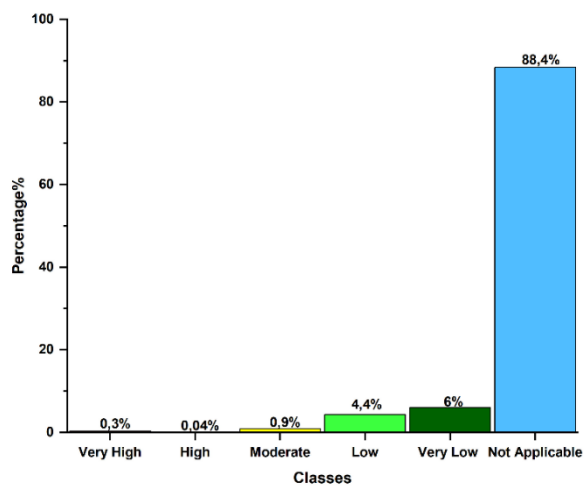
411 **Figure ~~141413~~. Damming Susceptibility Map of non-formation of river stretches by new landslides in**
412 **Tajikistan.** River network database from Coccia et al., (~~2023in-prep~~). Topographic base from NASA's SRTM
413 project (Far and Kobrick, 2000).



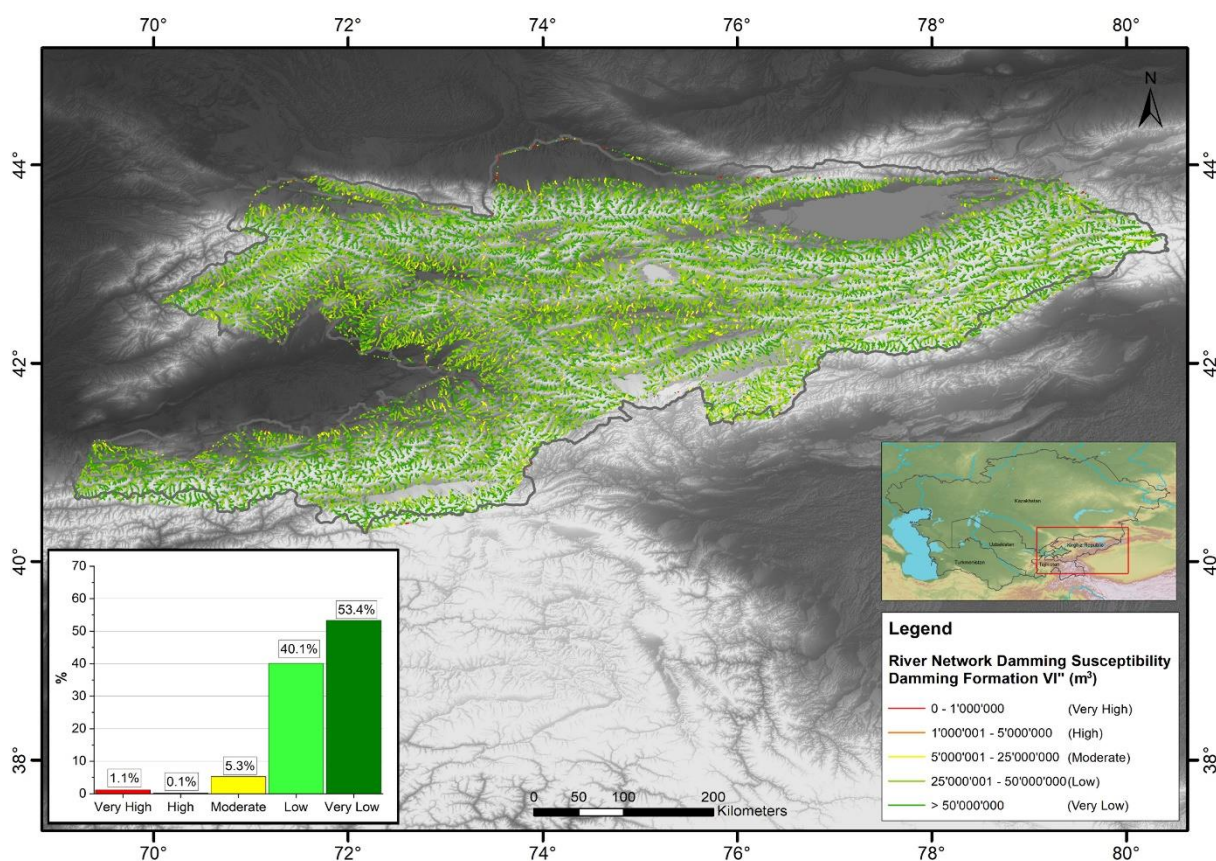
414

415 **Figure 151514. Damming Susceptibility Map of Formation of river stretches by new landslides in the**
 416 **region.** River network database from Coccia et al., ([in prep. 2023](#)). Basemap source: Esri, HERE, Garmin

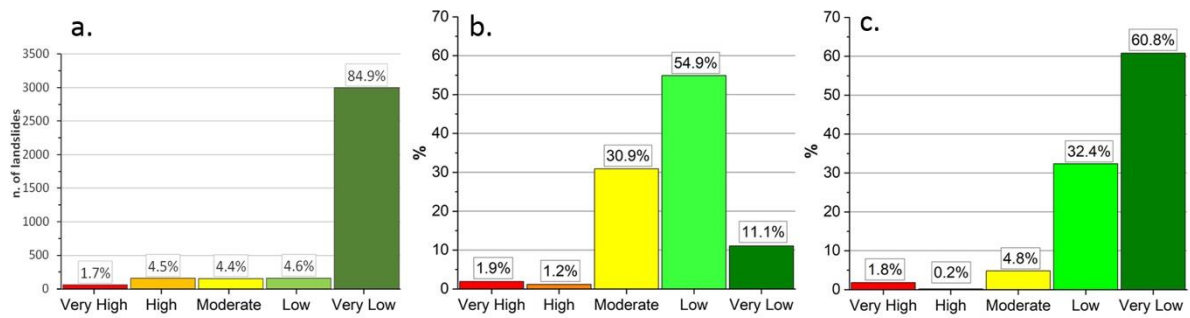
417 Intermap, increment P Corp, GEBCO, USGS, FAO, NPS, NRCAN, GeoBase, IGN, Kadaster NL, Ordnance
 418 Survey, Esri Japan, METI, Esri China (Honk Kong), © OpenStreetMap contributors, and the GIS User
 419 Community.



420
 421 **Figure 161615.** Distribution of the Damming Susceptibility in the study area by new landslides related to
 422 **Formation boundary values.**

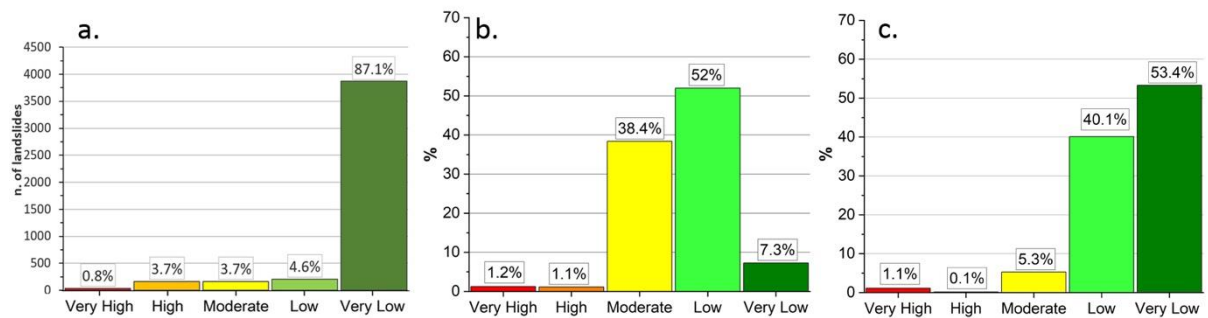


423
 424 **Figure 171716.** Damming Susceptibility Map of formation of river stretches by new landslides in the
 425 **Kyrgyz Republic territory.** River network database from Coccia et al., ([in prep-2023](#)). Topographic base from
 426 NASA's SRTM project (Far and Kobrick, 2000).



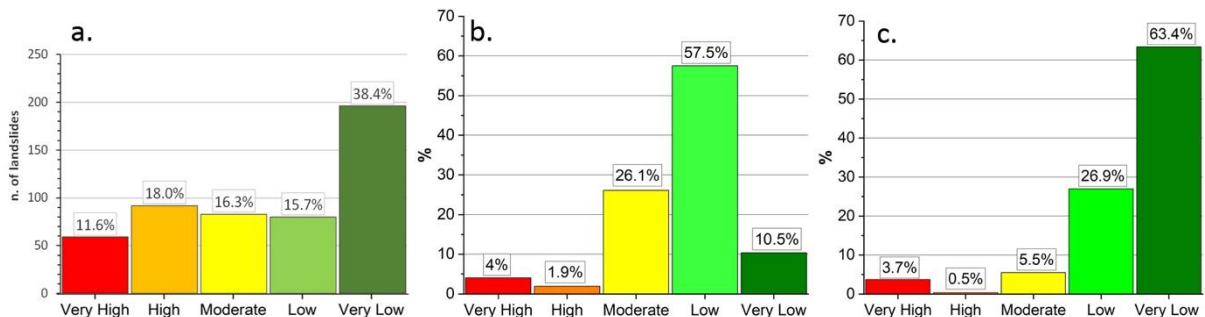
427

428 **Figure 181817.** Classes distribution in Tajikistan of the Damming Predisposition for landslides
 429 reactivation (a.), Damming Susceptibility of Non-Formation (b.) and of Formation (c.) for new landslides.



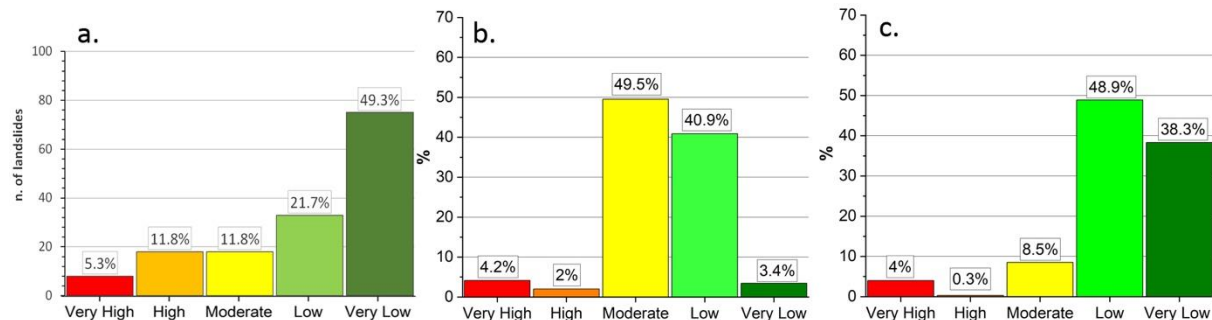
430

431 **Figure 191918.** Classes distribution in the Kyrgyz Republic of the Damming Predisposition for landslides
 432 reactivation (a.), Damming Susceptibility of Non-Formation (b.) and of Formation (c.) for new landslides.



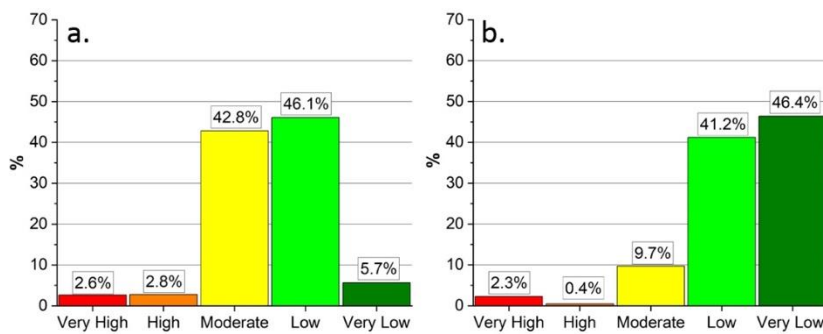
433

434 **Figure 202019.** Classes distribution in Uzbekistan of the Damming Predisposition for landslides
 435 reactivation (a.), Damming Susceptibility of Non-Formation (b.) and of Formation (c.) for new landslides.



436

437 **Figure 212120. Classes distribution in Kazakhstan of the Damming Predisposition for landslides**
 438 **reactivation (a.), Damming Susceptibility of Non-Formation (b.) and of Formation (c.) for new landslides.**



439
 440 **Figure 222221. Classes distribution in Turkmenistan of the Damming Susceptibility of Non-Formation (a.)**
 441 **and of Formation (b.) for new landslides.**

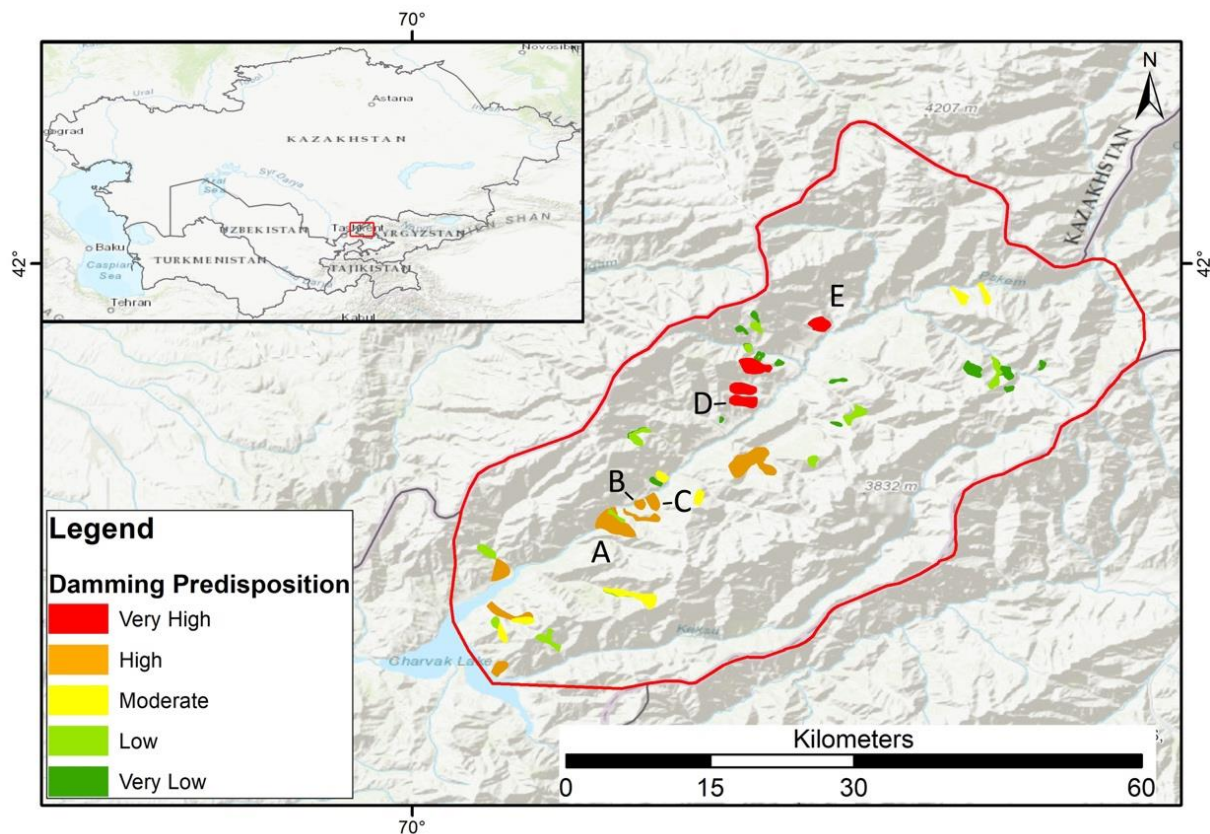
442 **4.1 Upper Pskem river valley (Uzbekistan)**

443 The Pskem river, locate in the Tashkent region of Uzbekistan, is a right-hand tributary of the Chirchik River that
 444 is the feeder of the Syr Darya river basin (in the Western Tien-Shan). The river originates from the confluence of
 445 the Maidantal and Oygaing rivers and is one of the main tributaries of the Charvak Lake (Semakova et al., 2016).
 446 This artificial lake is central for the local economy for its functions as reserve for fishing and water, as well as a
 447 source of hydroelectric energy and because of that various villages arise around it and downstream. The formation
 448 of a natural obstruction and an upstream impoundment in the Pskem basin could be a serious threat due to the
 449 possible instability of the earth dam and for the possible catastrophic cascade effects that its collapse could have
 450 downstream on the artificial basins and their 168 meters high earthfill dam.

451 With a careful observation of the map of Damming Predisposition by landslides reactivation in the lower Pskem
 452 basin in an area of 443 km² (Figure 23Figure 23Figure 22), some of the 53 mapped landslides should be subjected
 453 to further study. Among all, most landslides were classified with a Very Low and Low predisposition value,
 454 respectively 21 and 11 cases (39.6% and 20.8%), and only 4 landslides with a Very High value (7.5%), 10 with
 455 High (18.9%) and 7 with Moderate (13.2%). Landslides named A, B, C, D and E in Figure 23Figure 23Figure 22,
 456 if reactivated will potentially cause an obstruction of the main river section of the Pskem, being classified the first
 457 three and the latest two respectively with High and Very High damming predisposition. As shown in Table 2, the
 458 volumes of all these landslides are way bigger than the boundary volume of Non-Formation and Formation from
 459 Figure 24Figure 24Figure 23 and Figure 25Figure 25Figure 24. It is important to notice that the landslides A, B
 460 and C are laid down in the valley floor, meaning that in the past they had probably already dammed the river in
 461 that point, and the classification of their damming predisposition have been reduced by one, from Very High to
 462 High. Due to the considerable volumes of the landslides in the basin and the presence of landslides that have
 463 probably already blocked the river in the past, this relatively small area is certainly worthy of attention.

464 **Table 2. Landslides volumes and damming parameters W_v , V_1' , V_1'' of the landslides in Figure 20**
 465 **computed using the described method.**

Landslide	V_1 - Landslide volume (m ³)	W_v - River Width (m)	V_1' - Volume of Non-formation (m ³)	V_1'' - Volume of Formation (m ³)
A	200.000.000	300	2.600.000	16.200.000
B	12.000.000	235	1.500.000	10.000.000
C	34.000.000	318	3.000.000	18.200.000
D	73.000.000	513	10.100.000	47.400.000
E	61.000.000	575	13.500.000	60.000.000



466

467 **Figure 232322. Map of Damming Predisposition by landslides reactivation in the lower Pskem basin.**

468 Basemap source: Esri, HERE, Garmin Intermap, increment P Corp, GEBCO, USGS, FAO, NPS, NRCAN,
 469 GeoBase, IGN, Kadaster NL, Ordnance Survey, Esri Japan, METI, Esri China (Honk Kong), © OpenStreetMap
 470 contributors, and the GIS User Community.

471 The obstruction of the Pskem river by one of these landslides would cause an upstream impoundment with a
 472 surface from 2 to 10 km² or more, depending on the dam position and height. The dam collapse could release a
 473 catastrophic flooding wave with destructive effects in the downstream areas. In the worst scenario, even the
 474 earthfill dam located few kilometers downstream could be seriously damaged with unpredictable effects. Since the
 475 reliability of this mapping method is strictly correlated to the quality of the input data, when the used DEM has a
 476 coarse resolution, in similar cases of possible risk to people's life it is always advisable to do a second "manual
 477 check" even using some free satellite imaging services like Google Earth. In fact, when the DEM resolution is too
 478 rough, the GIS tool used in this methodology to evaluate the extension of the riverbed morphologic unit can

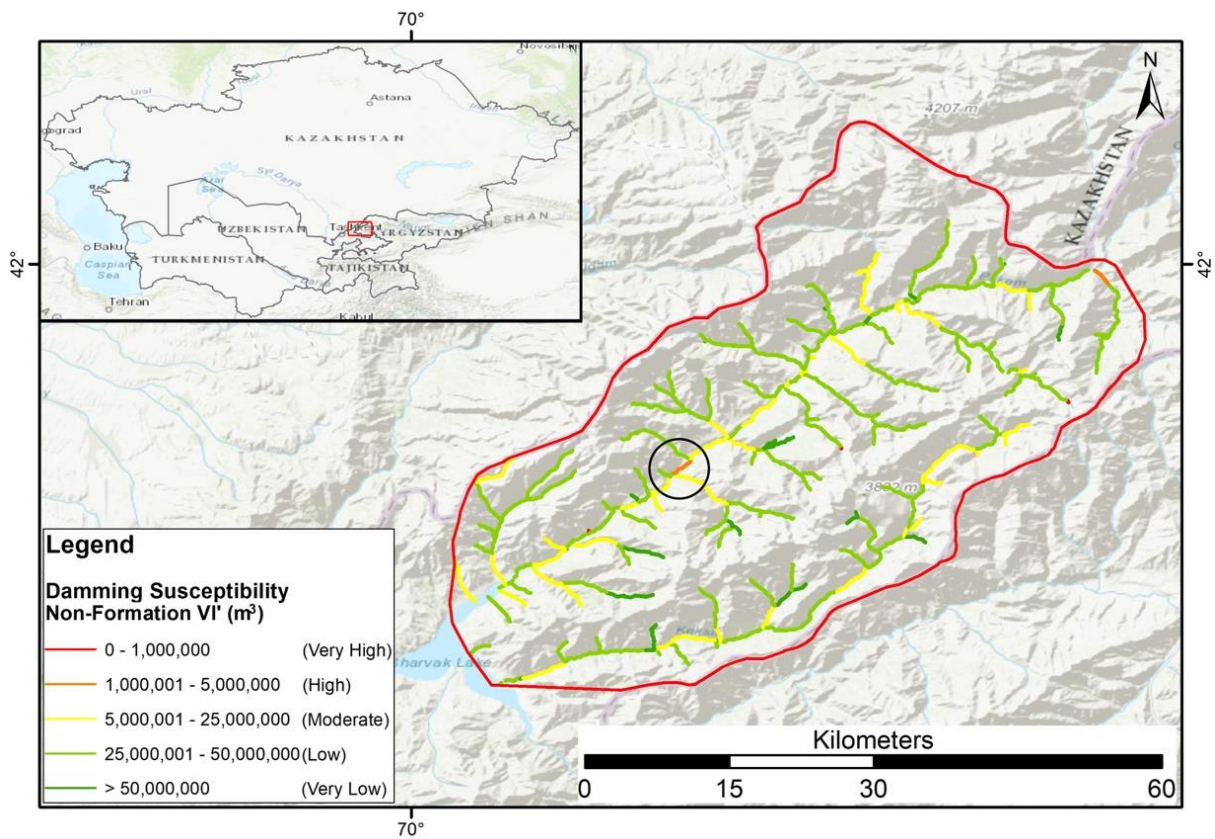
479 produce inconsistent and incorrect results, causing improper damming susceptibility evaluations. The results of
 480 the measurements on Google Earth orthophotos in Table 3 show that the difference between the river width values
 481 calculated with the mapping method (W_v) and those measured on Google Earth (W_{vGE}) can in some cases be
 482 substantial modifying the calculated boundary volumes V' and V'' , although in this case they do not modify
 483 drastically the final classification of the five landslides.

484 The river network of the upper Pskem valley have been also classified producing the maps of Damming
 485 Susceptibility of Non-formation and Formation ([Figure 24](#)~~Figure 24~~~~Figure 23~~ and [Figure 25](#)~~Figure 25~~~~Figure 24~~
 486 respectively). Concerning the Damming Susceptibility Map of Non-formation ([Figure 24](#)~~Figure 24~~~~Figure 23~~), the
 487 most frequent are Low and Moderate classes with 65.1% and 22.6% respectively, followed by Very Low class
 488 with 11.1%. Only just 1.3% have been classified as High and 0.0% as Very High. For the Damming Susceptibility
 489 Map of Formation ([Figure 25](#)~~Figure 25~~~~Figure 24~~) most of the rivers fall into Very Low and Low classes with
 490 69.8% and 27.7%, followed by Moderate class with 2.1%. Only 0.4% have been classified as High and 0.0% as
 491 Very High.

492 **Table 3. Damming parameters W_{vGE} , V'_{vGE} , V''_{vGE} of the landslides in [Figure 23](#)~~Figure 23~~~~Figure 22~~**
 493 **computed with Google Earth observation.**

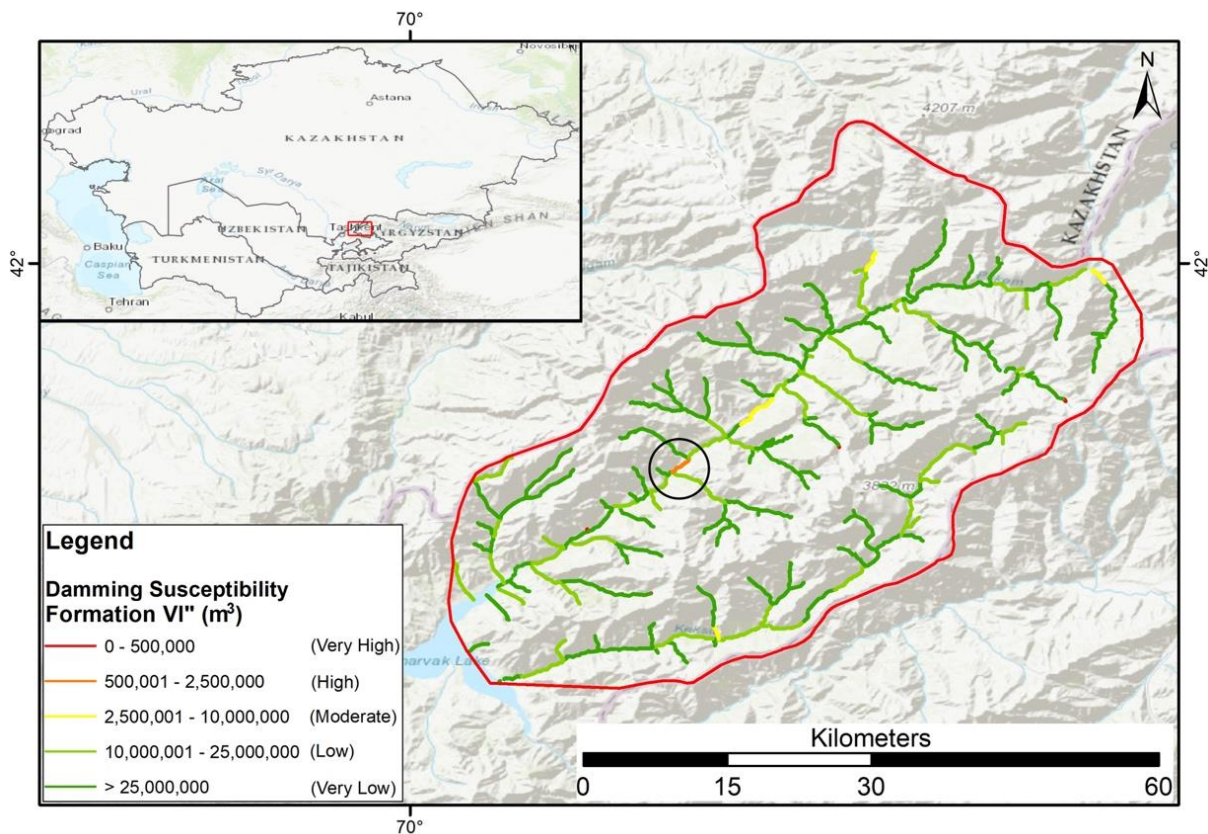
Landslide	W_{vGE} – River Width (m)	V'_{vGE} - Volume of non-formation (m ³)	V''_{vGE} - Volume of Formation (m ³)
A	415	6.000.000	31.000.000
B	310	2.800.000	17.300.000
C	260	1.800.000	12.100.000
D	530	11.000.000	50.000.000
E	450	7.300.000	36.500.000

494
 495 The general damming susceptibility of the valley is low but a singular river stretch, marked by a black circle in
 496 [Figure 24](#)~~Figure 24~~~~Figure 23~~ and [Figure 25](#)~~Figure 25~~~~Figure 24~~, classified with High susceptibility in both maps
 497 should be carefully evaluated. This river part is clearly noticeable in the middle of the area along the main river
 498 path, a bit upstream from the landslides named B and C. The high classification values mean that geographically
 499 in that point the valley width undergoes a shrinkage and for this reason even a relatively small landslide generated
 500 from the surrounding slopes can create an obstruction, therefore it would be worthy of a more detailed
 501 investigation.



502

503 **Figure 242423. Damming Susceptibility Map of Non-formation of river stretches by new landslides in the**
 504 **lower Pskem basin. The black circle highlights a river stretch with unusually high values.** River network
 505 database from Coccia et al., ([in-prep-2023](#)). Basemap source: Esri, HERE, Garmin Intermap, increment P Corp,
 506 GEBCO, USGS, FAO, NPS, NRCAN, GeoBase, IGN, Kadaster NL, Ordnance Survey, Esri Japan, METI, Esri
 507 China (Honk Kong), © OpenStreetMap contributors, and the GIS User Community.



528

529 **Figure 252524. Damming Susceptibility Map of Formation of river stretches by new landslides in the**
 530 **lower Pskem basin. The black circle highlights a river stretch with unusually high values.** River network
 531 database from Coccia et al., ([in-prep-2023](#)). Basemap source: Esri, HERE, Garmin Intermap, increment P Corp,
 532 GEBCO, USGS, FAO, NPS, NRCAN, GeoBase, IGN, Kadaster NL, Ordnance Survey, Esri Japan, METI, Esri
 533 China (Honk Kong), © OpenStreetMap contributors, and the GIS User Community.

534 4.2 The Fergana valley mountainous rim (Tajikistan-Kyrgyz Republic- 535 Uzbekistan)

536 The Fergana valley is one of the largest intermountain depressions in Central Asia located between Uzbekistan,
 537 Kyrgyz Republic, and Tajikistan. It hosts two main rivers, the Naryn and the Kara Darya, which join together to
 538 form the Syr Darya. In this populated area landslide activity is recurrent, causing every year damage to
 539 infrastructure and loss of human life, and triggered by complex interactions between multiple factors such as
 540 tectonic, geological, morphological and meteorological (Danneels et al., 2008; Schlöegel et al., 2011; Piroton et
 541 al., 2020). The mapping methodology have been applied also to the Fergana valley and a total of 3370 landslides,
 542 coming from various data sources, have been classified as shown in [Figure 26Figure 26Figure 25](#). Comparably to
 543 the classification result of the entire inventory ([Figure 9Figure 9Figure 8](#)) most of the cases (94%) have a Very
 544 Low damming predisposition, followed by Low and Moderate (with 2.5% and 1.8% respectively) as reported in
 545 [Table 4Table 4Table 4](#). Just very few landslides fall into High and Very High classes (with 1.4% and 0.3%
 546 respectively). For the classification of the river network of the Fergana valley, the maps of Damming Susceptibility
 547 of Non-formation and Formation have been produced ([Figure 27Figure 27Figure 26](#) and [Figure 28Figure 28Figure](#)

ha forma

566 [27](#) respectively). As a method with a multi-scale approach, in such large areas, this damming susceptibility method
 567 is suitable to provide territorial planning suggestions rather than indications on single interventions at local scale.
 568 The overall damming predisposition of the Fergana valley is quite low, considering the presence of 3370 mapped
 569 landslides in total, even if there are few landslides (10) classified with Very High damming predisposition which
 570 should be studied with more attention through localized analysis of damming susceptibility to ensure that
 571 downstream areas are not at risk and therefore require a specific monitoring.

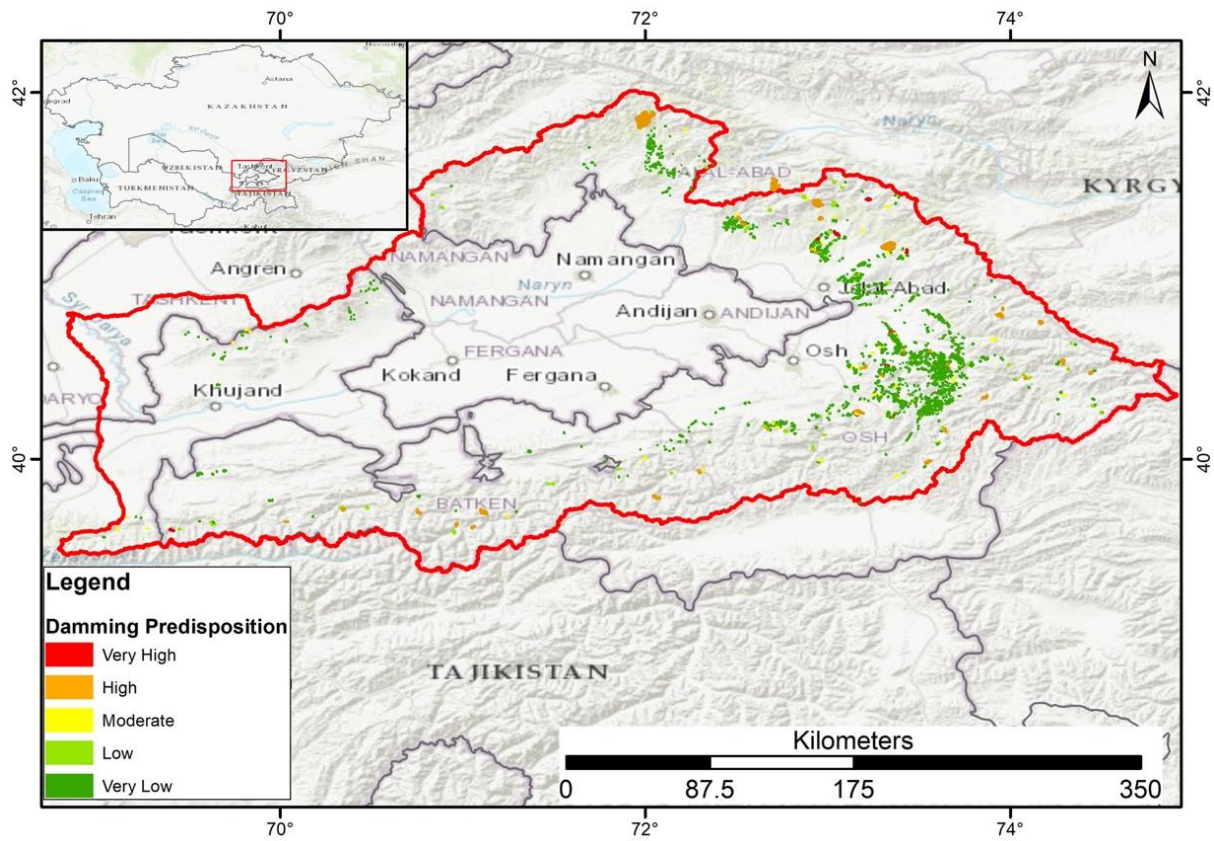
572 [Table 4](#)[Table 4](#)[Table 4](#) have been reported the distribution of the percentages of the damming susceptibility classes
 573 of those river stretches that are not running in flat areas, since these lowland rivers represent 53.6% of the total.
 574 Concerning the Damming Susceptibility Map of non-formation of the remaining river stretches ([Figure 27](#)[Figure](#)
 575 [27](#)[Figure 26](#)), the most frequent are Low and Moderate classes with 53.4% and 36.2% respectively, followed by
 576 Very Low class with 7.0%. Only just 2.1% and 1.3% have been classified as Very High and High. For the
 577 Damming Susceptibility Map of Formation ([Figure 28](#)[Figure 28](#)[Figure 27](#)) most of the rivers fall into Very Low
 578 and Low classes with 54.5% and 38.1%, followed by Moderate class with 5.2%. Only 1.9% and 0.2% have been
 579 classified as Very High and High respectively.

580 **Table 4. Distribution of Damming Susceptibility classes on existing landslides ([Figure 26](#)[Figure 26](#)[Figure](#)**
 581 **[25](#)) and on the river stretches for non-formation ([Figure 27](#)[Figure 27](#)[Figure 26](#)) and Formation of new**
 582 **landslides ([Figure 28](#)[Figure 28](#)[Figure 27](#)).**

Damming Susceptibility	Landslides		non-formation	Formation
	n.	%	%	%
Very High	10	0.3%	1.9	1.7
High	48	1.4%	1.2	0.2
Moderate	61	1.8%	7.0	5.3
Low	83	2.5%	53.2	38.8
Very Low	3168	94.0%	6.7	54.0

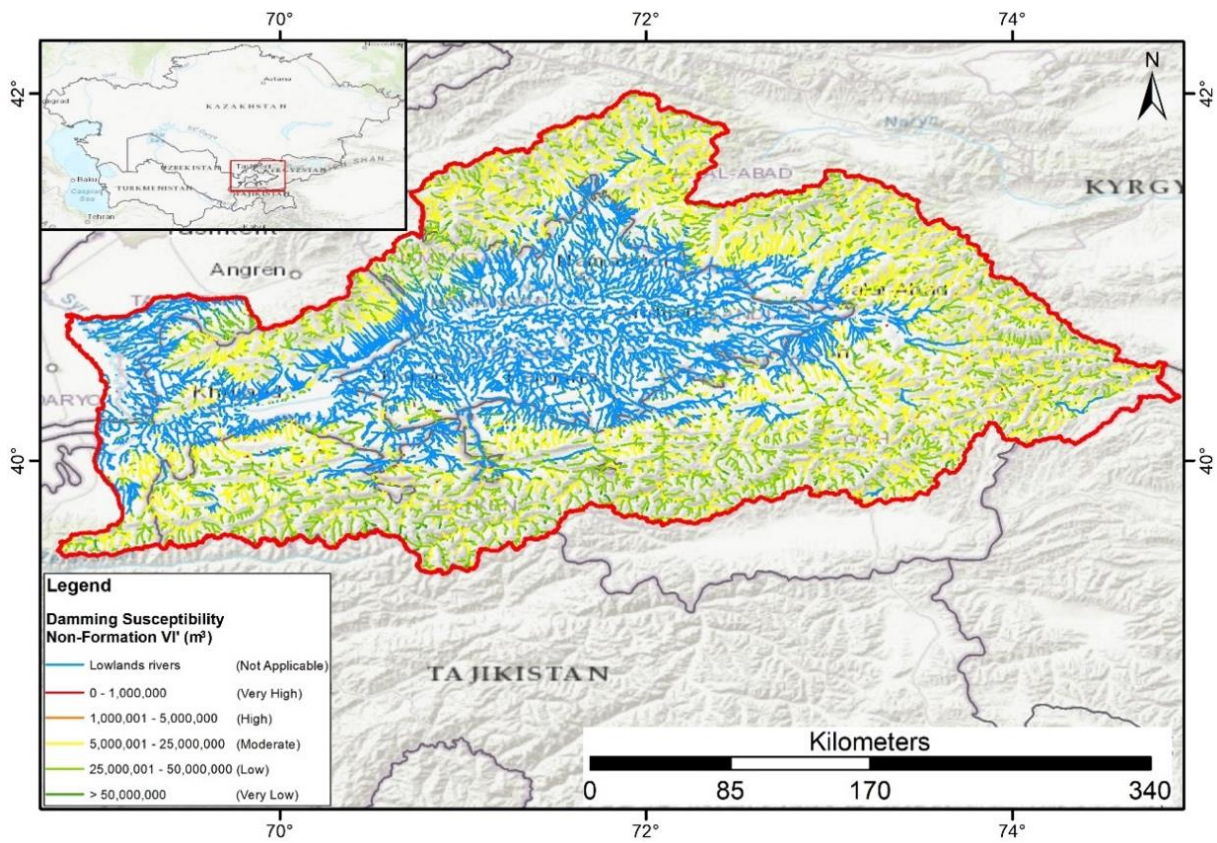
583

ha forma



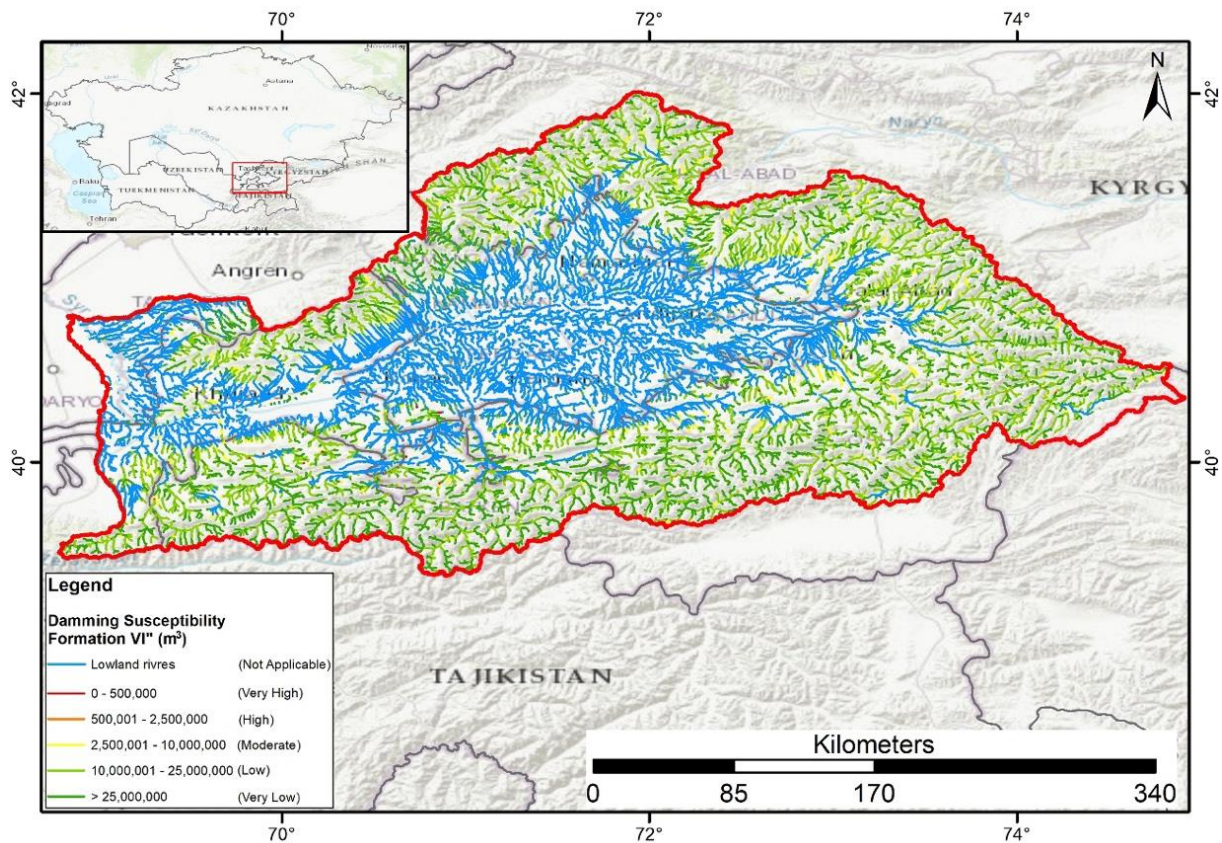
584

585 **Figure 262625. Map of Damming Predisposition by landslides reactivation in the Fergana valley.** Basemap
 586 source: Esri, HERE, Garmin Intermap, increment P Corp, GEBCO, USGS, FAO, NPS, NRCAN, GeoBase, IGN,
 587 Kadaster NL, Ordnance Survey, Esri Japan, METI, Esri China (Honk Kong), © OpenStreetMap contributors,
 588 and the GIS User Community.



589

590 **Figure 272726. Damming Susceptibility Map of Non-formation of river stretches by new landslides in the**
 591 **Fergana valley.** River network database from Coccia et al., ([in prep. 2023](#)). Basemap source: Esri, HERE,
 592 Garmin Intermap, increment P Corp, GEBCO, USGS, FAO, NPS, NRCAN, GeoBase, IGN, Kadaster NL,
 593 Ordnance Survey, Esri Japan, METI, Esri China (Honk Kong), © OpenStreetMap contributors, and the GIS User
 594 Community.



595

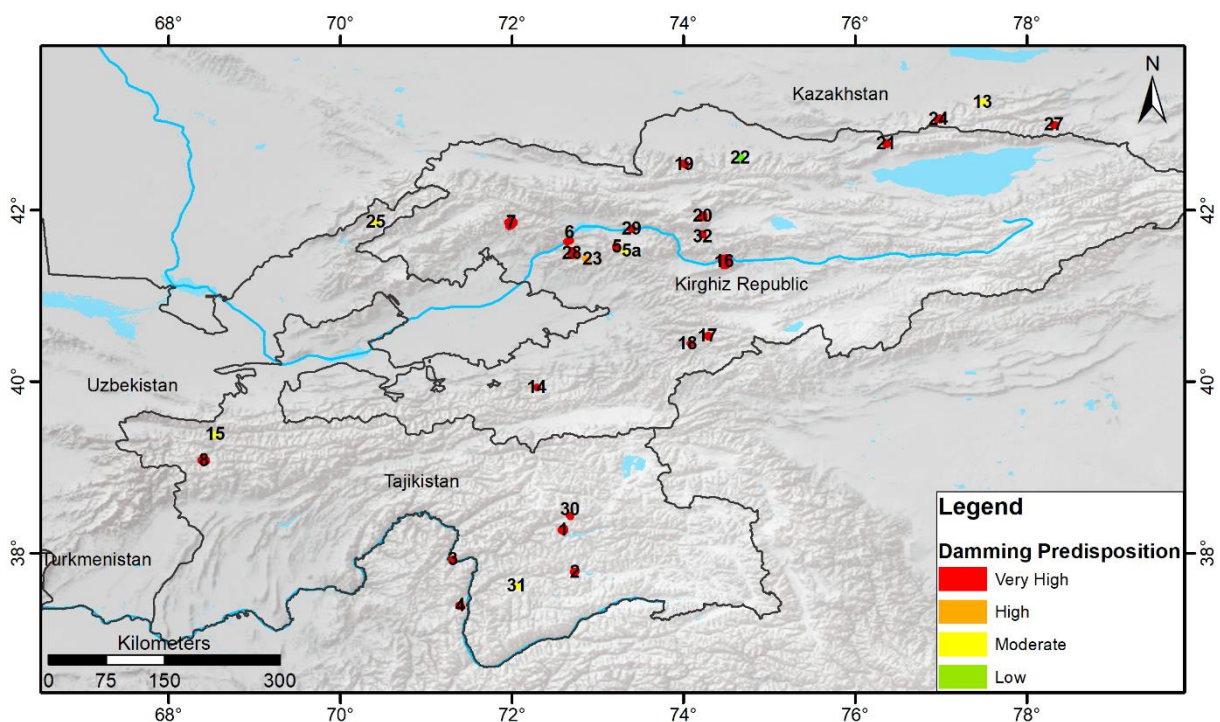
596 **Figure 282827. Damming Susceptibility Map of Formation of river stretches by new landslides in the**
 597 **Fergana valley.** River network database from Coccia et al., ([in prep.2023](#)). Basemap source: Esri, HERE,
 598 Garmin Intermap, increment P Corp, GEBCO, USGS, FAO, NPS, NRCAN, GeoBase, IGN, Kadaster NL,
 599 Ordnance Survey, Esri Japan, METI, Esri China (Honk Kong), © OpenStreetMap contributors, and the GIS User
 600 Community.

601 **5 Discussion**

602 During the application of the damming mapping methodology, the main issues encountered was the extremely
 603 wide study area, the amount of data and the processing time required. The used mapping methodology based on
 604 the MOI equations (Eq.(1)), was originally designed to assess the damming susceptibility at basin/regional scale
 605 (Tacconi Stefanelli et al., 2016; 2020), where the morphological parameters essential for the correct application of
 606 the tool proposed by Wood (2009) must be correctly found to have an accurate river width required in the MOI
 607 equations (Eq.(1)). This time-consuming phase has been simplified in this research, according to the wide
 608 dimension of the study area, taking into account not the basins but the different states in the Central Asia region.
 609 This simplification certainly affected the reliability of the individual specific data, while still guaranteeing an
 610 important overview of the general hazard distribution of the phenomenon in the area. Furthermore, the results
 611 quality is directly proportional to the resolution and quality of the input data, which on the other hand is inversely
 612 proportional to the processing time. In this regard, a further criticality of this process is the reliability on the
 613 landslides volumes assessment method, since a higher quality of landslides data (sliding geometry and depth)
 614 allows the application of a more accurate volume calculation and therefore a better final result.

615 Thus, even if the results are not always highly reliable at local scale, requiring many in-depth specific studies in
616 the areas identified with the higher predisposition, they can be undoubtedly useful in very large countries to adopt
617 risk reduction measures, for planning purposes and for land development management.

618 Considering the size of the area, in ~~Figure 11~~ ~~Figure 11~~ ~~Figure 10~~ the number of landslides classified with Very
619 High damming predisposition (166 cases) is reasonable in absolute value, even if a bit high if compared with the
620 total number of landslides present in the inventory (8910 cases). Without a detailed study it is not possible to say
621 how many of these are false positives or not, however it is important to remember that this type of hazard risk
622 mapping methods gives information on if and where, not when these events may occur. Although a validation of
623 all the results is not possible, we can verify some of these through comparison with cases known in the, as shown
624 in Figure 29. These landslides have been documented in Strom (2010) who has reported several landslide dams
625 in Central Asia regions. In Table 5 their current conditions are compared with their Damming Predisposition
626 classification using the methodology proposed here (before the intensity reduction of the classification by one
627 class of those landslides that intersect the river network). From this information can be observe that 23 (77% of
628 the total) of these landslides were correctly classified with the Very High predisposition value, 1 (3%) as High
629 and 5 (17%) with Moderate. Only one landslide, No. 22 called Arashan in Strom (2010), was classified as Low
630 predisposition despite it obstructed the Alamedin River and then collapsed and deeply eroded. This classification
631 error can be explained by the missing landslide volume eroded by the river as a bigger value would probably
632 have provided a higher predisposition. Based on this simple comparison, approximately 80% of the landslide
633 dams analysed by Strom (2010) has a corrected Damming Predisposition value (Very High) based on their
634 volume and the width of their valley. The final classification value of Damming Predisposition of all of them has
635 been downgraded by one class as they intersect the river network (see Section 3 Materials and Methods).



636

641 **Figure 29. Map of Damming Predisposition using landslide from Strom (2010).** See Table 5 for landslide
 642 [numbers](#). Lake's polygons from Esri, Garmin International, Inc.; basemap from Esri, USGS, NOAA.

643 **Table 5. Information of landslides in Figure 29 (from Strom, 2010) and their Damming Predisposition**
 644 **assessment.**

<u>N.</u>	<u>Name</u>	<u>Mountain chain-Region</u>	<u>Consequences</u>	<u>Damming Predisposition</u>
<u>1</u>	<u>Usoi</u>	<u>Pamirs-Tajikistan</u>	<u>Dammed (with lake)</u>	<u>Very High</u>
<u>2</u>	<u>Yashilkul</u>	<u>Pamirs-Tajikistan</u>	<u>Dammed (with lake)</u>	<u>Very High</u>
<u>3</u>	<u>Shids</u>	<u>Pamirs-Tajikistan</u>	<u>Dammed (with lake, partially breached)</u>	<u>Very High</u>
<u>4</u>	<u>Shiva</u>	<u>Pamirs-Afghanistan</u>	<u>Dammed (with lake)</u>	<u>Very High</u>
<u>5</u>	<u>Karasu</u>	<u>Tien Shan-Kyrgyz Rep.</u>	<u>Dammed (with lake)</u>	<u>Very High</u>
<u>5a</u>	<u>Kapkatash</u>	<u>Tien Shan-Kyrgyz Rep.</u>	<u>Dammed (with lake)</u>	<u>Moderate</u>
<u>6</u>	<u>Karakul</u>	<u>Tien Shan-Kyrgyz Rep.</u>	<u>Dammed (filled lake)</u>	<u>Very High</u>
<u>7</u>	<u>Sarychelek</u>	<u>Tien Shan-Kyrgyz Rep.</u>	<u>Dammed (with lake)</u>	<u>Very High</u>
<u>8</u>	<u>Iskanderkul</u>	<u>Tien Shan-Tajikistan</u>	<u>Dammed (with lake)</u>	<u>Very High</u>
<u>9</u>	<u>Tianchi</u>	<u>Tien Shan-China</u>	<u>Dammed (with lake)</u>	<u>Very High</u>
<u>11</u>	<u>Twin-Lakes (upper)</u>	<u>Tien Shan-China</u>	<u>Dammed (with lake)</u>	<u>Very High</u>
<u>12</u>	<u>Twin-Lakes (lower)</u>	<u>Tien Shan-China</u>	<u>Dammed (with lake)</u>	<u>Very High</u>
<u>13</u>	<u>Issyk</u>	<u>Tien Shan-Kazakhstan</u>	<u>Dammed (with lake)</u>	<u>Moderate</u>
<u>14</u>	<u>Yashinkul</u>	<u>Tien Shan-Kyrgyz Rep.</u>	<u>Dammed (collapsed)</u>	<u>Very High</u>
<u>15</u>	<u>Aini</u>	<u>Tien Shan-Tajikistan</u>	<u>Dammed (lake artificially drained)</u>	<u>Moderate</u>
<u>16</u>	<u>Beshkiol</u>	<u>Tien Shan-Kyrgyz Rep.</u>	<u>Dammed (collapsed)</u>	<u>Very High</u>
<u>17</u>	<u>Kulun</u>	<u>Tien Shan-Kyrgyz Rep.</u>	<u>Dammed (with lake)</u>	<u>Very High</u>
<u>18</u>	<u>Kulun Mouth</u>	<u>Tien Shan-Kyrgyz Rep.</u>	<u>Dammed (filled lake)</u>	<u>Very High</u>
<u>19</u>	<u>Aksu</u>	<u>Tien Shan-Kyrgyz Rep.</u>	<u>Dammed (collapsed)</u>	<u>Very High</u>
<u>20</u>	<u>Kokomeren</u>	<u>Tien Shan-Kyrgyz Rep.</u>	<u>Dammed (collapsed)</u>	<u>Very High</u>
<u>21</u>	<u>Djashilkul</u>	<u>Tien Shan-Kyrgyz Rep.</u>	<u>Dammed (collapsed)</u>	<u>Very High</u>
<u>22</u>	<u>Arashan</u>	<u>Tien Shan-Kyrgyz Rep.</u>	<u>Dammed (collapsed)</u>	<u>Low</u>
<u>23</u>	<u>Kutmankul</u>	<u>Tien Shan-Kyrgyz Rep.</u>	<u>Dammed (with lake)</u>	<u>High</u>
<u>24</u>	<u>Bolshoe Almaty</u>	<u>Tien Shan-Kazakhstan</u>	<u>Dammed (with lake)</u>	<u>Very High</u>
<u>25</u>	<u>Badak</u>	<u>Tien Shan-Uzbekistan</u>	<u>Dammed (with lake)</u>	<u>Moderate</u>
<u>28</u>	<u>Dead Lakes</u>	<u>Tien Shan-Kyrgyz Rep.</u>	<u>Dammed (with lake)</u>	<u>Very High</u>

29	<u>Djuzumdybulak</u>	<u>Tien Shan-Kyrgyz Rep.</u>	<u>Dammed (with lake)</u>	<u>Very High</u>
30	<u>Kudara</u>	<u>Pamirs-Tajikistan</u>	<u>Dammed (collapsed)</u>	<u>Very High</u>
31	<u>Rivakkul</u>	<u>Pamirs-Tajikistan</u>	<u>Dammed (with lake)</u>	<u>Moderate</u>
32	<u>Ornok</u>	<u>Tien Shan-Kyrgyz Rep.</u>	<u>Dammed (collapsed)</u>	<u>Very High</u>

645

646 The two maps of damming susceptibility (~~Figure 12~~~~Figure 12~~~~Figure 14~~ and ~~Figure 15~~~~Figure 15~~~~Figure 14~~), while
647 not providing probability values as done by Tacconi Stefanelli et al. (2020), offer information (the volumes of
648 landslides) that can be more easily spent and interpreted even by operators who are not specifically expert, and for
649 this reason have more practical utility. Furthermore, the classification of the river stretches thus produced, not
650 requiring the alpha parameter (linked to the probability of landslide occurrence) as in the original method proposed
651 by Tacconi Stefanelli et al. (2020), it is much easier to obtain and for this reason it can be considered an
652 improvement within a view of wider usability.

643 6 Conclusions

654 The price of a river obstruction, in terms of reconstruction and losses on both economic and lives, can be much
655 higher compared with the costs of a proper environmental planning and land-use management. Be able to define
656 the areas with higher risk could considerably lower the costs, allowing to focus the economic resources in effective
657 preventive interventions, planning and monitoring activities.

658 In this work a damming mapping methodology have been proposed and carried out on the Central Asia regions as
659 a part of a multi-hazard approach in the framework of the SFRARR Project (“Strengthening Financial Resilience
660 and Accelerating Risk Reduction in Central Asia”). The used method, originally developed applying the
661 Morphological Obstruction Index at basin scale, have been modified to fit such a large study area and the available
662 data. ~~The improvement of the original method allows a simpler use and the need for less data, more easily available,~~
663 ~~although the absence of a validation of the results inevitably remains.~~ Over 8000 landslides and the entire river
664 network of studied area have been analyzed ~~The main aim of this study was~~ to propose a practical tool to assess
665 where the damming susceptibility, from reactivation of mapped landslides and formation of new landslides, are
666 higher at national scale. The improvement of the original method allows a simpler use on a wider area, as the
667 technical knowledge and data required can also be managed by a non-expert operator, and the need for less data,
668 more easily available. The main limitation of the work is related to the uncertainty of the reliability of the results
669 at local scale due to the absence of a possible validation of all results, requiring many in-depth specific studies in
670 the areas identified with the higher predisposition. This uncertainty can be improved in future studies by using
671 data with better resolution, coverage, and quality.

672 Besides its limitations, this tool can be undoubted useful in very large countries where there is a lack of diffuse
673 assessment of landslide activity, providing preliminary information about damming susceptibility to adopt risk
674 reduction measures, for land management and as a starting point for future studies in specific areas potentially
675 more subject to the damming hazard identified in this work.~~This second result of the mapping damming~~

676 ~~susceptibility from new landslide can be particularly useful in area of the world where there is a lack of diffuse~~
677 ~~assessment of landslide activity and incomplete landslide inventories.~~

678 **Code and data availability.** The landslide dam mapping susceptibility method was implemented by using the cited
679 landslide inventory maps, published by the following authors: Behling et al., 2014, 2016, 2020; Havenith et al.,
680 2015a; Strom and Abdrakhmatov, 2018. The SRTM DEM data are available from <https://earthexplorer.usgs.gov/>.
681 The river network and other landslide inventories were provided by the SFRAAR project partners: RED (Risk,
682 Engineering + Development – Pavia, Italy), OGS (National Institute of Oceanography and Experimental
683 Geophysics, Seismological Research Center, Trieste, Italy), IWPHE (Institute of Water problems, Hydropower,
684 Engineering and Ecology, Dushanbe, Republic of Tajikistan), ISASUZ (Institute of Seismology of the Academy
685 of Science of Uzbekistan, Tashkent, Uzbekistan), LLP (Institute of Seismology of the Science Committee of the
686 Republic of Kazakhstan, Almaty).

687 **Author contribution.** Carlo Tacconi Stefanelli implemented the damming mapping method, William Frodella
688 conceived with Carlo Tacconi Stefanelli the article structure and collected the data, Francesco Caleca supported
689 the method application on part of the study area. Francesco Caleca also performed statistical analysis involving
690 the method results. All the aforementioned Authors contributed to the writing of the article and the figure graphics.
691 Veronica Tofani coordinated the work and reviewed the paper. Zhanar Raimbekova and Ruslan Umuraliev
692 provided environment and geomorphology information and part of the landslide database for Kazakhstan and
693 Kyrgyz Republic.

694 **Competing interests.** The contact author has declared that none of the authors has any competing interests.

695 **Acknowledgements.** This work was developed within World Bank-funded project “*Strengthening Financial*
696 *Resilience and Accelerating Risk Reduction in Central Asia*” (SFRARR), in collaboration with the European
697 Union, and the GFDRR (Global Facility for Disaster Reduction and Recovery), with the goal of improving
698 financial resilience and risk-informed investment planning in the central Asian countries (Kazakhstan, Kyrgyz
699 Republic, Tajikistan, Turkmenistan and Uzbekistan). This work brings the part of the results of the Task 7
700 “Landslide Scenario Assessment”, managed by the UNESCO Chair on Prevention and Sustainable Management
701 of Geo-Hydrological Hazards (University of Florence, Italy). In particular, the authors would like to thank Gabriele
702 Coccia and Paola Ceresa from Red Risk Engineering (Pavia, Italy) for providing river network data and for the
703 valuable coordination and constant support, and also Alexander Strom and Hans Balder Havenith for providing
704 landslide inventories and for their constructive advice and valuable observations. We would also like to thank the
705 partners from Central Asia for the fruitful collaboration, in particular: IWPHE (Tajikistan), ISASUZ and the State
706 Monitoring Service of the Republic of Uzbekistan for tracking dangerous geological processes (Uzbekistan), the
707 Institute of Seismology of the National Academy of Sciences of Kyrgyz Republic (ISNASKR), and the Institute
708 of Seismology Limited Liability Partnership (LLP) of Kazakhstan.

709 **Financial support.** This research has been supported by the World Bank Group (Consulting Services Contract No.
710 8006611 – Regionally consistent risk assessment for earthquakes and floods and selective landslide scenario
711 analysis for strengthening financial resilience and accelerating risk reduction in Central Asia).

712 **References**

- 713 Abdrakhmatov, K.Y., Aldazhanov, S.A., Hager, B.H., Hamburger, M.W., Herring, T.A., Kalabaev, K.B.,
714 Makarov, P. Molnar, S.V. Panasyuk, M.T. Prilepin, R.E. Reilinger, I.S. Sadybakasov, B.J. Souter, Yu.A.
715 Trapeznikov, V.Ye., and Tsurkov Zubovich, A.V.: Relatively recent construction of the Tien Shan inferred
716 from GPS measurements of present-day crustal deformation rates. *Nature*, 384(6608), 450-45319, 1996.
- 717 Abdrakhmatov, K., Havenith, H.B., Delvaux, D., Jongmans, D., and Trefois, P.: Probabilistic PGA and Arias
718 Intensity Maps of Kyrgyz Republic (Central Asia). *J. Seismol.* 7.2: 203-220, 2003. ~~Akgun, A. A comparison
719 of landslide susceptibility maps produced by logistic regression, multi-criteria decision, and likelihood ratio
720 methods: A case study at İzmir, Turkey. *Landslides* 2012, 9, 93–106.~~
- 721 ~~Bazzurro, P. et al.: Strengthening Financial Resilience and Accelerating Risk Reduction in Central Asia—the
722 SFRARR project. The SFRARR probabilistic flood hazard assessment, in preparation, 2023.~~
- 723 Behling, R., Roessner, S., Kaufmann, H., and Kleinschmit, B.: Automated spatiotemporal landslide mapping over
724 large areas using rapideye time series data. *Remote Sens.* 6, 8026–8055, 2014.
- 725 Behling, R., Roessner, S., Golovko, D., and Kleinschmit, B.: Derivation of long-term spatiotemporal landslide
726 activity—A multi-sensor time series approach. *Remote Sens. Environ.* 186, 88–104, 2016.
- 727 Behling, R., and Roessner, S.: Multi-temporal landslide inventory for a study area in Southern Kyrgyz Republic
728 derived from RapidEye satellite time series data (2009 – 2013). V. 1.0. GFZ Data Services.
729 <https://doi.org/10.5880/GFZ.1.4.2020.001>, 2020.
- 730 Borgatti, L., and Soldati, M.: Landslides as a geomorphological proxy for climate change: a record from the
731 Dolomites (northern Italy), *Geomorphology*, 120(1–2), 56–64, 2010.
- 732 CAC DRMI: Risk assessment for Central Asia and Caucasus: desk study review, 2009.
- 733 Canuti, P., Casagli, N., Ermini, L., Fanti, R., and Farina, P.: Landslide activity as a geoinicator in Italy:
734 significance and new perspectives from remote sensing, *Environ. Geol.*, 45(7), 907–919, 2004.
- 735 Casagli, N., and Ermini, L.: Geomorphic analysis of landslide dams in the Northern Apennine, *Trans. Jpn.*
736 *Geomorphol. Union.*, 20(3), 219–249, 1999.
- 737 Catani, F., Tofani, V., and Lagomarsino, D.: Spatial patterns of landslide dimension: a tool for magnitude mapping,
738 *Geomorphology* 273, 361–373. <https://doi.org/10.1016/j.geomorph.2016.08.032>, 2016.
- 739 Chedia, O.K., and Lemzin, I.N.: Seismogenerating faults of the Chatkal depression. In: *Seismotectonics and*
740 *seismicity of the Tien Shan*. Frunze, Ilim, 18–28, 1980.
- 741 ~~[Chen, C. Y., Chang, J. M.: Landslide dam formation susceptibility analysis based on geomorphic features.](#)
742 [Landslides](#), 13(5), 1019-1033, 2016.~~
- 743 ~~[Coccia, G., Ceresa, P., Bussi, G., Denaro, S., Bazzurro, P., Martina, M., Fagà, E., Avelar, C., Ordaz, M., Huerta,](#)
744 [B., Garay, O., Raimbekova, Z., Abdrakhmatov, K., Mirzokhonova, S., Ismailov, V., and Belikov, V.: Large-](#)
745 [scale flood risk assessment in data scarce areas: an application to Central Asia.](#) *Nat. Hazards Earth Syst. Sci.*~~

746 [Discuss. \[preprint\], https://doi.org/10.5194/nhess-2023-157](https://doi.org/10.5194/nhess-2023-157), in review, 2023. ~~Cocchia, G. et al.: The SFRARR~~
747 ~~probabilistic flood hazard assessment, NHES, in preparation, 2023.~~
748

749 Costa, J.E., and Schuster, R.L.: Documented historical landslide dams from around the world. US Geol. Surv.
750 Open-File Report, 91(239), 1-486, 1991.

751 [Costa, J.E., and Schuster, R.L.: Formation and failure of natural dams. Bull Geol Soc Am, 100 \(7\), 1054–1068.](https://doi.org/10.0016-1988)100/0016-7606(1988)100<1054:TFAFON>2.3.CO.1988)
752 [https://doi.org/10.0016-1988\)100/0016-7606\(1988\)100<1054:TFAFON>2.3.CO.1988.](https://doi.org/10.0016-1988)100/0016-7606(1988)100<1054:TFAFON>2.3.CO.1988)

753 Crozier, M.J.: Deciphering the effect of climate change on landslide activity: a review, *Geomorphology*, 124(3),
754 260–267, 2010.

755 [Dai, F. C., Lee, C. F., Deng, J. H., Tham, L. G.: The 1786 earthquake-triggered landslide dam and subsequent](https://doi.org/10.1016/j.geomorph.2005.03.005)
756 [dam-break flood on the Dadu River, southwestern China. *Geomorphology*, 65\(3\), 205-221, 2005.](https://doi.org/10.1016/j.geomorph.2005.03.005)

757 Dal Sasso, S.F., Sole, A., Pascale, S., Sdao, F., Bateman Pinzòn, A., and Medina, V.: Assessment methodology
758 for the prediction of landslide dam hazard, *Nat. Hazards Earth Syst. Sci.*, 14 (3), 557–567,
759 <http://dx.doi.org/10.5194/nhess-14-557-2014>, 2014.

760 Danneels, G., Bourdeau, C., Torgoev, I., Havenith, H. B. Geophysical investigation and dynamic modelling of
761 unstable slopes: case-study of Kainama (Kyrgyzstan). *Geophys. J. Int.*, 175(1), 17-34, 2008.

762 Delvaux, D., Abdrakhmatov, K.E., Lemzin, I.N., and Strom, A.L.: Landslides and surface breaks of the 1911 Ms
763 8.2 Kemin earthquake, Kyrgyzstan, *Russian Geology and Geophysics*, 2001, 42, 10, 1667-1677, 2001.

764 Dikau, R., and Schrott, L.: The temporal stability and activity of landslides in Europe with respect to climatic
765 change (TESLEC): main objectives and results, *Geomorphology*, 30(1–2), 1–12, 1999.

766 Drăguț, L., and Dornik, A.: Land-surface segmentation as a method to create strata for spatial sampling and its
767 potential for digital soil mapping, *Int. J. Geogr. Inf. Sci.*, 30(7), 1359-1376, 2016.

768 [Ermini, L., Casagli, N.: Prediction of the behavior of landslide dams using a geomorphical dimensionless index,](https://doi.org/10.1002/esp.424)
769 [Earth Surf Proc Land 28:31–47. https://doi.org/10.1002/esp.424, 2003.](https://doi.org/10.1002/esp.424)

770 [Falátková, K.: Temporal analysis of GLOFs in high-mountain regions of Asia and assessment of their causes,](https://doi.org/10.1016/j.aucgeo.2016.02.001)
771 [AUC Geographica, 51, 2, 145–154, 2016.](https://doi.org/10.1016/j.aucgeo.2016.02.001)

772 Fan, X., Rossiter, D.G., van Westen, C.J., Xu, Q., and Görüm, T.: Empirical prediction of coseismic landslide dam
773 formation, *Earth. Surf. Proc. Land.*, 39(14), 1913–1926, 2014.

774 Fan, X., Dufresne, A., Subramanian, S.S., Strom, A., Hermanns, R., Tacconi Stefanelli, C., Hewitt, K., Yunus,
775 A.P., Dunning, S., Capra, L., Geertsema, M., Miller, B., Casagli, N., Jansen, J.D., and Xu, Q.: The formation
776 and impact of landslide dams – State of the art, *Earth Sci. Rev.*, 203, 103116,
777 <https://doi.org/10.1016/j.earscirev.2020.103116>, 2020.

778 Fan, X., Dufresne, A., Whiteley, J., Yunus, A. P., Subramanian, S.S., Okeke, C. A., Pánek, T., Hermanns, R.,
779 Ming, P., Strom, A., Havenith, H.-B., Dunning, S., Wang, G., and Tacconi Stefanelli, C.: Recent

780 technological and methodological advances for the investigation of landslide dams, *Earth-Sci. Rev.*, 218,
781 103646, <https://doi.org/10.1016/j.earscirev.2021.103646>, 2021.

782 Farr, T.G., and Kobrick, M.: Shuttle Radar Topography Mission produces a wealth of data. *Eos Trans. AGU*, 81,
783 583-583, 2000.

784 Golovko, D., Roessner, S., Behling, R., Wetzel, H. U., and Kleinschmidt, B.: Development of multi-temporal
785 landslide inventory information system for southern Kyrgyz Republic using GIS and satellite remote sensing,
786 *PFG*, 2015(2), 157–172, 2015.

787 Guzzetti, F., Ardizzone, F., Cardinali, M., Rossi, M., and Valigi, D.: Landslide volumes and landslide mobilization
788 rates in Umbria, central Italy, *EPSL*, 279, 222–229, 2009.

789 Havenith, H.B., Strom, A., Cacerez, F., and Pirard, E.: Analysis of landslide susceptibility in the Suusamyр region,
790 Tien Shan: statistical and geotechnical approach. *Landslides* 3, 39–50, 2006a.

791 Havenith, H.B., Torgoev, I., Meleshko, A., Alioshin, Y., Torgoev, A., and Danneels, G.: Landslides in the Mailuu-
792 Suu Valley, Kyrgyz Republic—hazards and impacts, *Landslides*, 3, 137–147, 2006b.

793 Havenith, H.B., Strom, A., Torgoev, I., Torgoev, A., Lamair, L., Ischuk, A., and Abdrakhmatov, K.: Tien Shan
794 geohazards database: Earthquakes and landslides, *Geomorphology*, 249, 16–31, 2015a.

795 Havenith, H.B., Torgoev, A., Schlögel, R., Braun, A., Torgoev, I., and Ischuk, A.: Tien Shan geohazards database:
796 Landslide susceptibility analysis, *Geomorphology*, 249, 32–43, 2015b.

797 Havenith, H.B., Umaraliev, R., Schlögel, R., Torgoev, I., Ruslan, U., Schlogel, R., and Torgoev, I.: Past and
798 Potential Future Socioeconomic Impacts of Environmental Hazards in Kyrgyz Republic. In *Kyrgyz Republic:
799 Political, Economic and Social Issues*; Olivier, A.P., Ed.; Nova Science Publishers, Inc.: Hauppauge, NY,
800 USA; pp. 63–113, 2017.

801 Hungr, O., and Evans, S.G.: Entrainment of debris in rock avalanches: an analysis of a long run-out mechanism,
802 *Geol. Soc. Am. Bull.*, 116(9-10), 1240-1252, 2004.

803 [Juliev, M., Pulatov, A., and Hubl, J.: Natural hazards in mountain regions of Uzbekistan: A review of mass](#)
804 [movement processes in Tashkent province. *International Journal of Scientific and Engineering Research*,](#)
805 [8\(2\), 1102, 2017.](#)

806 Kalmetieva, Z.A., Mikolaichuk, A.V, Moldobekov, B.D., Meleshko, A. V, Janaev, M.M., and Zubovich, A.V.:
807 Atlas of earthquakes in Kyrgyz Republic. Central-Asian Institute for Applied Geosciences and United
808 Nations International Strategy for Disaster Reduction Secretariat Office in Central Asia, Bishkek, p 75, 2009.

809 [King, J., Loveday, I., Schuster, R. L.: The 1985 Bairaman landslide dam and resulting debris flow, *Papua New*](#)
810 [Guinea. *Q J Eng Geol Hydroge.* 22\(4\), 257-270, 1989.](#)

811 [Kropáček, J., Vilímek, V. & Mehrishi, P.: A preliminary assessment of the Chamoli rock and ice avalanche in the](#)
812 [Indian Himalayas by remote sensing, *Landslides*, 18, 3489–3497, \[https://doi.org/10.1007/s10346-021-\]\(https://doi.org/10.1007/s10346-021-01742-1\)](#)
813 [01742-1, 2021.](#)

814 Liao, H. M., Yang, X. G., Lu, G. D., Tao, J., and Zhou, J. W.: A geotechnical index for landslide dam stability
815 assessment, *Geomatics, Natural Hazards and Risk*, 13(1), 854-876,
816 <https://doi.org/10.1080/19475705.2022.2048906>, 2022.

817 Maxwell, A.E., and Shobe, C.M.: Land-surface parameters for spatial predictive mapping and modeling, *Earth-*
818 *Sci. Rev.*, 226, 103944, 2022.

819 Molnar, P., and Tapponnier, P.: Cenozoic Tectonics of Asia: Effects of a Continental Collision: Features of recent
820 continental tectonics in Asia can be interpreted as results of the India-Eurasia collision. *science*, 189(4201),
821 419-426, 1975.

822 Niyazov, R.A.: Uzbekistan landslides. Uzbekistan landslide service. Technical report, 2020.

823 [Peresan, A., Scaini, C., Tyagunov, S., and Ceresa, P.: Capacity Building Experience for Disaster Risk Reduction](#)
824 [in Central Asia, *Nat. Hazards Earth Syst. Sci. Discuss.* \[preprint\], <https://doi.org/10.5194/nhess-2023-156>, in](#)
825 [review, 2023.](#)

826 Petrov, M.A., Sabitov, T.Y., Tomashevskaya, I.G., Glazirin, G.E., Chernomorets, S.S., Savernyuk, E.A.,
827 Tutubalina O.V., Petrakov, D.A., Sokolov, L.S., Dokukin, M.D., Mountrakis, G., Ruiz-Villanueva, V., and
828 Stoffel, M.: Glacial lake inventory and lake outburst potential in Uzbekistan, *Sci. Total Environ.*, 592, 228-
829 242, 2017.

830 Piroton, V., Schlögel, R., Barbier, C., and Havenith, H.B.: Monitoring the recent activity of landslides in the
831 Mailuu-suuy valley (Kyrgyz Republic) using radar and optical remote sensing techniques. *Geosciences*, 10
832 (5), p. 164, 2020.

833 Popescu, M.E., and Sasahara, K.: Engineering Measures for Landslide Disaster Mitigation, in: *Landslides –*
834 *Disaster Risk Reduction*, edited by: Sassa, K., Canuti, P., Springer, Berlin, Heidelberg, 609-631,
835 https://doi.org/10.1007/978-3-540-69970-5_32, 2009.

836 Righini, M., and Surian, N.: Remote sensing as a tool for analysing channel dynamics and geomorphic effects of
837 floods, *Flood monitoring through remote sensing*, 27-59, 2018.

838 Rosi, A., Frodella, W., Nocentini, N., Caleca, F., Havenith, H.B., Strom, A., Saidov, M., Bimurzaev, G.A., and
839 Tofani, V.: Comprehensive landslide susceptibility map of Central Asia, *Nat. Hazards Earth Syst. Sci.*, 23,
840 2229–2250, <https://doi.org/10.5194/nhess-23-2229-2023>, 2023.

841 Saponaro, A., Pilz, M., Wieland, M., Bindi, D., Moldobekov, B., and Parolai, S.: Landslide susceptibility analysis
842 in data-scarce regions: the case of Kyrgyz Republic. *Bull. Eng. Geol. Environ.* 74, 1117–1136, 2014.

843 Schlögel, R., Torgoev, I., De, Marneffe, C., and Havenith, H.B.: Evidence of a changing size-frequency
844 distribution of landslides in the Kyrgyz Tien Shan, Central Asia. *Earth Surf Process Landf* 36(12), 1658–
845 1669, 2011.

846 Schuster, R.L., and Evans, S.G.: Engineering Measures for the Hazard Reduction of Landslide Dams, in: *Natural*
847 *and Artificial Rockslide Dams. Lecture Notes in Earth Sciences*, edited by: Evans, S., Hermanns, R., Strom,

848 A., Scarascia-Mugnozza, G., Springer, Berlin, Heidelberg, https://doi.org/10.1007/978-3-642-04764-0_2,
849 2011.

850 Semakova, E., Gunasekara, K., and Semakov, D.: Identification of the glaciers and mountain naturally dammed
851 lakes in the Pskem, the Kashkadarya and the Surhandarya River basins, Uzbekistan, using ALOS satellite
852 data, *Geomat. Nat. Hazards Risk*, 7(3), 1081-1098, 2016.

853 Strom, A.: Landslide dams in Central Asia region. *Journal of the Japan Landslide Society*, 47(6), 309-324, 2010.

854 Strom, A., and Abdrakhmatov, K.: Large-Scale Rockslide Inventories: From the Kokomeren River Basin to the
855 Entire Central Asia Region (WCoE 2014–2017, IPL-106-2, in: Workshop on World Landslide Forum.
856 Springer, Cham, pp. 339–346, 2017.

857 Strom, A., and Abdrakhmatov, K.: Rockslides and rock avalanches of Central Asia: distribution, morphology, and
858 internal structure. Elsevier, 441pg. ISBN: 978-0-12-803204-6, 2018.

859 Swanson, F.J., Oyagi, N., and Tominaga, M.: Landslide dams in Japan, in: *Landslide dams: processes, risk and*
860 *mitigation*, vol 3, edited by: Schuster R.L., Geotech. Sp., ASCE, New York, 131–145, 1986.

861 Tacconi Stefanelli, C., Catani, F., Casagli, N.: Geomorphological investigations on landslide dams. *Geoenviron Disast*
862 2(1):1–15. <https://doi.org/10.1186/s40677-015-0030-9>, 2015.

863 Tacconi Stefanelli, C., Segoni, S., Casagli, N., and Catani, F.: Geomorphic indexing of landslide dams evolution,
864 *Eng. Geol.*, 208, 1–10. <https://doi.org/10.1016/j.enggeo.2016.04.024>, 2016.

865 Tacconi Stefanelli, C., Vilímek, V., Emmer, A., and Catani, F.: Morphological analysis and features of the
866 landslide dams in the Cordillera Blanca, Peru, *Landslides*, 15(3), 507-521, [https://doi.org/10.1007/s10346-](https://doi.org/10.1007/s10346-017-0909-5)
867 [017-0909-5](https://doi.org/10.1007/s10346-017-0909-5), 2018.

868 Tacconi Stefanelli, C., Casagli, N., and Catani, F.: Landslide damming hazard susceptibility maps: a new GIS-
869 based procedure for risk management, *Landslides*, 17, 1635-1648, [https://doi.org/10.1007/s10346-020-](https://doi.org/10.1007/s10346-020-01395-6)
870 [01395-6](https://doi.org/10.1007/s10346-020-01395-6), 2020.

871 Trifonov, V.G., Makarov, V.I., and Scobelev, S.F.: The Talas-Fergana active right-slip faults. *Ann Tectonicae*
872 6:224–237, 1992.

873 Ullah, S., Bindi, D., Pilz, M., Danciu, L., Weatherill, G., Zuccolo, E., Anatoly Ischuk, A., Mikhailova, N.N.,
874 Abdrakhmatov, K., and Parolai, S. Probabilistic seismic hazard assessment for Central Asia. *Annals of*
875 *Geophysics*, 58(1), 2015.

876 Wang, X., Ding, Y., Liu, S., Jiang, L., Wu, K., Jiang, Z., and Guo, W.: Changes of glacial lakes and implications
877 in Tian Shan, central Asia, based on remote sensing data from 1990 to 2010, *Environ. Res. Lett.*, 8(4),
878 044052, 2013.

879 Wang, D., Laffan, S.W., Liu, Y., and Wu, L.: Morphometric characterization of landform from DEMs, *Int. J.*
880 *Geogr. Inf. Sci.*, 24(2), 305–326, 2010.

- 881 Wood, J.: Geomorphometry in LandSerf. In: Hengl, T. and Reuter, H.I. [Eds.]: Geomorphometry: Concepts,
882 Software, Applications, Dev. Soil. Sci., 33, 333-349, 2009.
- 883 Zubovich, A. V., Wang, X. Q., Scherba, Y. G., Schelochkov, G. G., Reilinger, R., Reigber, C., Mosienko, O.,
884 Molnar, P., Michajljow, W., Makarov, V.I., Li, J., Kuzikov, S.I., Herring, T.A., Hamburger, M.W., Hager
885 B.H., Dang, Y., Bragin, V.D., and Beisenbaev, R.: GPS velocity field for the Tien Shan and surrounding
886 regions. *Tectonics*, 29(6), 2010.